

1  
2 Prof. Jim Freer  
3 Editor  
4 Hydrology and Earth System Sciences

5 February 20<sup>th</sup>, 2015

6 Dear Prof. Freer,

7

8 We would like to acknowledge the revision of our work originally entitled “Uncertainty propagation in  
9 a cascade modelling approach to flood mapping”. We thank you for your constructive comments, which  
10 in addition to the previous comments from the reviewers very much helped to improve our manuscript.

11 We have digested the comments you pointed out concerning the discussion of our work, and in  
12 consequence made considerable changes to our manuscript. I would like to draw your attention to the  
13 improvement of the rainfall-runoff model description, which now incorporates details with regards its  
14 calibration and use within the framework.

15 We made an effort to incorporate precise changes in the manuscript that acknowledged the raised points.  
16 Please note that as in the previous revision, following the suggestion of reviewer two, the title was  
17 changed to: **Propagation of hydro-meteorological uncertainty in a model cascade framework to**  
18 **inundation prediction.**

19 In the following lines we explain how (i.e. by writing our reply in red) and where (i.e. by giving line  
20 numbers) each point of your comments have been incorporated in the revised manuscript. We hope that  
21 this new version proves to be of interest to you and the reviewers and that it is worth to be considered  
22 for publication in HESS.

23

24 Best wishes,

25

26

27 Dr. Adrián Pedrozo-Acuña on behalf of all authors

28

29 PS. We are very sorry for your loss.

30

1 **Editor Initial Decision: Reconsider after major revisions (12 Jan 2015) by Dr. Jim Freer**

2 **Comments to the Author:**

3 I thank both the reviewers and the authors for their responses. There are a few of matters to consider to  
4 allow this paper to be published in HESS and to be completed in a major revision. Some points on  
5 which the reviews have covered and one or two I feel must be better addressed in the manuscript.

6 **R: We thank Prof. Freer for leaving the door open for the possible publication of this work in HESS.  
7 This study represents the first of its kind in Mexico, and we are very thankful not only for the given  
8 opportunity but also for the raised points, which we believe have served us well in the improvement of  
9 the manuscript.**

10 My comments on this discussion phase are as follows:

11 1) Novelty – Reviewer 1 brings up the issue of a lack of perceived novelty about the paper. As I stated  
12 in my initial assessment I feel the paper is ‘novel’ in the sense there are very few papers that have  
13 cascaded results through from the meteorology. However the reporting is quite basic and in lack lacks  
14 scientific rigour in a number of respects. Not all have been fully teased out by the review process  
15 including:

16 **R: Once more, thank you to the editor for noting that the novelty of the approach lies in the sense there  
17 are very few papers that have cascaded results through from the meteorology. Our objective is not to  
18 accurately reproduce what was observed during this event, but to study how errors in the initial stage  
19 of the model cascade propagate towards the prediction of flood extension. As it will be explained in  
20 the following response we have made major improvements aiming at a better reporting of what was  
21 done.**

22 a) There really is a complete lack of detail how the models have each been run/calibrated. This must  
23 be improved significantly including the rational behind using certain parameter/model structure/etc.  
24 limits and ranges and techniques to evaluate them

25 **R: With this regard, modifications in the sections corresponding to the three modelling stages have been  
26 incorporated as follows:**

27 ***Meteorological model:*** In order to analyze the propagation of simulation errors originated at the initial  
28 stage of the model chain, the use of a multi-physics ensemble was thought to generate results with a  
29 highly varying skill to observations. No weighting or rejection functions were employed as the purpose  
30 of the study is precisely to analyze how errors propagate, in contrast to the development of an accurate  
31 model chain. An explicit acknowledgement to this fact appears now at Page 8 Lines 1-13.

32 ***Hydrological Model:*** With regards to this step of the model cascade, several changes have been  
33 incorporated. Firstly, a better description of the model appears at Page 10 Lines 11- Page 11 Line 3.  
34 Following the criticism of the selection of fixed free parameters in the hydrological model (i.e.  
35 deterministic), we have incorporated the definition of six sets of parameters that adequately reproduce  
36 flood hydrographs observed in past events (2001, 2005, 2007, 2008 and 2011). The definition of these  
37 parameters has been made through the implementation of a traditional calibration process for each of  
38 these events. This enabled the determination of equally valid parameters to reproduce the 2009 flood  
39 hydrograph (see new Table 3). These parameters in combination with the 12 members of the multi-  
40 physics ensemble gave way to the generation of 72 possible hydrographs for the 2009 flood. However,

1 as the purpose of this study is to investigate how errors in the meteorological prediction stage propagate  
2 down to a predicted inundation, the skill of hydrological predictions was limited by selecting only those  
3 with a  $Cor > 0.7$  and  $NSC > 0.6$ . The explanation for this procedure appears now at Page 11 Line 4 – Page  
4 12 Line 19.

5 Inundation model: The section associated to the flood inundation model has been enriched with a  
6 discussion on the justification of selected friction values, which appears in Page 13 Line 22 – Page 14  
7 Line 6. Additionally, a discussion on the apparent good skill of the simulated inundation extents has  
8 been included and appears at Page 15 Lines 9 -27.

9 b) The authors seem to have no clear grasp of how the resultant uncertainties/sensitivity to final  
10 propagated outputs is reliant on their experimental design. In that they clearly choose a set of WRF  
11 outputs that have highly varying skill to observations but include no weighting function (or even  
12 rejection) of these outputs.

13 R: As stated before, the use of a multi-physics ensemble was thought to generate results with a highly  
14 varying skill to observations. No weighting or rejection functions were employed as the purpose of the  
15 study is precisely to analyze how errors propagate, in contrast to the development of an accurate model  
16 chain. See Page 8 Lines 1-13.

17 Then there is such limited information on the hydrological model it's difficult to determine what was  
18 done (and similar comments could be made for the inundation extent). The issue here is their core  
19 conclusion is based on the fact that 'uncertainty does not increase'. Well that might be the case but  
20 without a sensible and rationale approach to the limits for each modelling component in the cascade  
21 this is not an outcome that can be justified. The paper is very weak in this regard and must be  
22 significantly improved. For example it isn't rationale to me to have an ensemble of input uncertainties  
23 but then seemingly use a completely deterministic hydrological model and then suggest the  
24 uncertainties do not increase, this is not exploring an uncertain cascade and the conclusions cannot be  
25 justified from it (and again in the flooding part of the modelling this is deterministic). Finally just to  
26 drive this point home it seems difficult that the authors in their conclusions then recognise that models  
27 are an imperfect representation (so how can single structure/parameter combinations be justified?). I  
28 would also argue the 'epistemic' nature of the WRF outputs, given observed knowledge of the system  
29 was available, was not evaluated sensibly in a probabilistic/uncertainty approach such as others have  
30 done.....

31 R: In order to take these comments into account, several modifications to the manuscript have been  
32 incorporated. These are mainly summarized as follows:

- 33 i. We have obtained 72 hydrographs from the combination of 12 multi-physics  
34 parameterizations in the WRF model with 6 sets of parameters in the hydrological model. This  
35 has been done to avoid the traditional deterministic use of the hydrological model, however, a  
36 full GLUE methodology was not deemed necessary as the main aim of the study is to  
37 propagate uncertainties originated in the meteorological model. For this reason, we have  
38 reduced the number of possible hydrographs from 72 to 31 (that comply with  $Cor > 0.7$  and  
39  $NSC > 0.6$ ).
- 40 ii. A new graph explaining the sensitivity of final propagated outputs is shown in Figure 9, where  
41 the relationship between the flood peak discharge and their corresponding maximum- flooded  
42 areas is incorporated. Results suggest that despite the variability in peak discharge the  
43 majority of hydrographs determine a flood extension of similar magnitude (see histograms in

1 Figure 9b and c). A discussion of these results has been included in Page Page 14, lines 22-  
2 31.

3 iii. With regards to the statement “uncertainty does not increase”, we have deleted it following the  
4 analysis of new computations and results (incorporating inundation depths), that have shed  
5 light on a complex aggregation of errors to the output. This is verified in the observed  
6 sensitivity of the simulated inundation depths (see Figure 10), where the geomorphology of  
7 the floodplain appears to be dominant in the flood extent determination. This is precisely our  
8 case, as small changes in lateral flood extent produced large changes in water levels.  
9 However, due to the lack of inundation depths data, we could not assess model performance  
10 using this information.

11 c) The authors fail to discuss properly the dynamics of the inundated area and how much this is a  
12 valley filling event (so perhaps a lack of sensitivity to inundation area changes would be expected). So  
13 are other dynamics in the model changing (like simulated depths?). I also feel there needs to be much  
14 better processing of the SPOT images to show the ‘observed’ extent of the flooding and to effectively  
15 relate that to the simulated extent. This is not adequately done at the moment

16 R: Thank you for noting this, we have carried out an analysis of flood dynamics both in horizontal (flood  
17 extension) and vertical (flood depths) dimensions. We concur that the sensitivity of the foremost features  
18 of the inundation: area and depth should be examined in this work. For such reasons, in Figure 10, we  
19 show the distribution of the maxima inundation depths at different locations across the floodplain. It can  
20 be observed that in most of the simulations, an upper limit (blue box, top with no visible bar) constrains  
21 the maxima inundation depths while the lower limit (blue box, both with visible bar) implies a lot of  
22 variability in the bottom maximum depth range. This is explained in the manuscript (Page 14, lines 26-  
23 31). Additionally, we have incorporated a discussion on how the case study fits the characteristics of a  
24 valley filling event at Page 15 Lines 1 – 8 and Lines 20-26.

25 Moreover, a revision of inundated depths is also presented and discussed. This appears at Page 15 Line  
26 27 – Page 16 Line 11.

27 Due to the coarse resolution of the SPOT image (124m) a better processing of the image to determine  
28 flood extent was not possible. No other image was available for its use. Under the light of the new results  
29 (Figure 9 and 10), pointing towards a similar flooded area for all model runs, the “observed” flood extent  
30 is not dominant to assess model performance.

31 I do agree with most, if not all, of the points raised by the reviewers. I think the response of the authors  
32 seems to be welcome (improving links to a wider range of research papers and improving readability  
33 and an understanding of what techniques have been deployed). If the authors cover these points well in  
34 a revised manuscript and include further work to address the points above then the revised paper will be  
35 considered for publication, but this might result in another round of discussion first as the changes are  
36 quite considerable.

37 R: We would like to warmly thank the referees for the observations and time spent during the review  
38 process. We believe that the incorporated analysis of uncertainty and sensitivity along the model cascade  
39 are reflected in this new version.

40 We have made considerable changes to our manuscript, hoping that this new version proves to be of  
41 interest to you and the referees.

42

# Uncertainty propagation Propagation of hydro- meteorological uncertainty in a model cascade modelling approach framework to inundation prediction

J. P. Rodríguez-Rincón<sup>1</sup>, A. Pedrozo-Acuña<sup>1\*</sup> and J. A. Breña-Naranjo<sup>1</sup>

[1]{National Autonomous University of México, Institute of Engineering, D.F., Mexico}

\*Correspondence to: A. Pedrozo-Acuña (APedrozoA@ii.unam.mx)

## Abstract

The purpose of this investigation is to study the propagation of meteorological uncertainty within a cascade modelling approach to flood mapping. The methodology iswas comprised of a Numerical Weather Prediction Model (NWP), a distributed rainfall-runoff model and a standard 2D hydrodynamic model. The cascade of models is used to reproduce an extreme flood event that took place in the Southeast of Mexico, during November 2009. The event iswas selected as high quality field data (e.g. rain gauges; discharge) and satellite imagery are available. Uncertainty in the meteorological model (Weather Research and Forecasting model) iswas evaluated through the use of a multi-physics ensemble technique, which considers twelve parameterization schemes to determine a given precipitation event. The resulting precipitation fields are used as input in a distributed hydrological model, enabling the determination of different hydrographs associated to this event. Lastly, by means of a standard 2D hydrodynamic model, flood hydrographs are used as forcing conditions to study the propagation of the meteorological uncertainty to an estimated flooded inundation area. Results show the utility of the selected modelling approach to investigate error propagation within a cascade of models. Moreover, the ~~error associated to the determination of the runoff, is showed to be lower than that obtained in the precipitation estimation suggesting that uncertainty do not necessarily increase within a model cascade~~ evolution of skill within the model cascade shows a complex aggregation of errors between models, suggesting that in valley-filling events hydro-meteorological uncertainty affects inundation depths in a higher degree than that observed in estimated flood extents.

1

2

### 3 **1 Introduction**

4 Hydro-meteorological hazards can have cascading effects and far-reaching implications on  
5 water security, with political, social, economic and environmental consequences. Millions of  
6 people worldwide are forcibly displaced as a result of natural disasters, creating political  
7 tensions and social needs to support them. These events observed in developed and developing  
8 nations alike, highlight the necessity to generate a better understanding on what causes them  
9 and how we can better manage and reduce the risk.

10 The assessment of flood risk is an activity that has to be carried out under a framework full of  
11 uncertainty. The source of these uncertainties may be ascribed to the involvement of different,  
12 and often rather complex models and tools, in the context of environmental conditions that are  
13 at best, partially understood (Hall, 2014). In addition to this, flooding ~~system~~events are  
14 dynamic over a range of timescales, due to ~~for example~~ climate variability and socio-economic  
15 changes, among others, which further increases the uncertainty in the projections. Therefore,  
16 numerous types of ~~uncertainty~~uncertainties can arise when using formal models in the analysis  
17 of risks.

18 Uncertainty is often categorised between aleatory and epistemic ~~uncertainty~~ (Hacking, 2006):  
19 aleatory is an essential, unavoidable unpredictability, and epistemic uncertainty reflects lack of  
20 knowledge or the inadequacy of the models to represent reality. In the context of any modelling  
21 framework, epistemic uncertainties may be ascribed to the definition of model parameters and  
22 to the model structure itself (limited knowledge).

23 In a technological era characterised by the advent of computers, there is an increased ability of  
24 more detailed hydrological and hydraulic models. Their use and development has been  
25 motivated as they are based on equations that have (more or less) physical justification; and  
26 allow a more detailed spatial representation of the processes, parameters and predicted variables  
27 (Beven, 2014). However, there are also disadvantages, these numerical tools take more  
28 computer time and require the definition of initial, boundary conditions and parameter values  
29 in space and time. Generally, at a level of detail for which such information is not available  
30 even in research studies. Moreover, these models may be ~~subjet~~subjected to numerical

1 problems such as numerical diffusion and instability. All of these disadvantages can be  
2 interpreted as sources of uncertainty in the modelling process.

3 Due to wide range of uncertainty sources in the flood risk assessment process, it is of great  
4 interest to investigate the propagation and behaviour of these different uncertainties from the  
5 start of the modelling framework to the result. The size of registered damages and losses in  
6 recent events around the world, reveal the urgency of doing so, even under a context of limited  
7 predictability.

8 In September 2013, severe floods were registered in Mexico as a result of the exceptional  
9 simultaneous incidence of two tropical storms, culminating in serious damage and widespread  
10 persistent flooding (Pedrozo-Acuña et al., 2014). ~~More recently, in 2014,2014a). This~~  
11 ~~unprecedented event is part of a recent set of extreme flood events over the last decade caused~~  
12 ~~by record-breaking precipitation amounts across Central Europe (Becker and flooding was~~  
13 ~~observed in the Grünewald, 2003).~~ United Kingdom (Slingo et al., 2014)-2014), Pakistan  
14 (Webster et al., 2011), Australia (Ven den Honert and McAneney, 2011), Northeastern US  
15 (WMO, 2011), Japan (WMO, 2011) and Korea (WMO, 2011). In ~~both~~all cases, the immediate  
16 action of governments through the implementation of emergency and action plans was required.  
17 The main aim of these interventions was to reduce the duration and impact of floods. In ~~both~~  
18 ~~events~~addition, risk reduction measures were designed to ensure both a better flood  
19 management and an increase in infrastructure resilience.

20 One key piece of information in preventing and reducing losses is given by reliable flood  
21 inundation maps that enable the dissemination of flood risk to the society and decision makers  
22 (Pedrozo-Acuña et al., 2013). Traditionally, this task requires the estimation of different return  
23 periods for discharge (Ward et al., 2011) and their propagation to the floodplain by means of a  
24 hydrodynamic model. There is currently a large range of models that can be used to develop  
25 flood hazard maps (Horrit and Bates, 2002; Horrit et al., 2006).

26 The aforementioned accelerated progress of computers has given way to the development of  
27 model cascades to produce hydrological forecasts, which make use of rainfall predictions from  
28 regional climate models (RCMs) with sufficient resolution to capture meteorological events  
29 (Bartholomes and Todini, 2005; Demerit et al., 2010). Within this approach, the coupling of  
30 different operational numerical models is carried out, using numerical weather prediction  
31 (NWP) with radar data for hydrologic forecast purposes (Liguori and Rico-Ramirez, 2012;

1 Liguori et al., 2012), or NWP with hydrological and hydrodynamic models to determine  
2 inundation extension (Pappenberger et al., 2012; Cloke et al., 2013; Ushiyama et al., 2014).

3 The use of RCMs in climate impact studies on flooding has been reported by Teutschbein and  
4 Seibert (2010) and Beven (2011), noting that despite their usefulness, the spatial resolution of  
5 models (~25km) remains coarse to capture the spatial resolution of precipitation. This is  
6 particularly important, as higher resolution is needed to effectively model the hydrological  
7 processes essential for determining flood risk. To overcome this limitation, the utilisation of  
8 dynamic downscaling in these models ~~is also~~ has been significantly growing (Fowler et al.,  
9 2007; Leung and Qian, 2009; Lo et al., 2008).

10 Significant challenges remain in the foreseeable future, among these, the inherent uncertainties  
11 in the predictive models ~~is~~ are likely to have an important role to play. For example, it is well  
12 known that the performance skill of NWP's deteriorates very rapidly with time (Lo et al., 2008).  
13 To overcome this, the long-term continuous integration of the prediction has been subdivided  
14 into short-simulations, involving the re-initialisation of the model to mitigate the problem of  
15 systematic error growth in long integrations (Giorgi, 1990; Giorgi, 2006; Qian et al., 2003).  
16 Moreover, the use of ensemble prediction systems to obtain rainfall predictions for hydrological  
17 forecasts at the catchment scale is becoming more common among the hydrological community  
18 as they enable the evaluation and quantification of some uncertainties in the results (Buizza  
19 2008; Cloke and Pappenberger, 2009; Bartholmes et al. 2009). In these studies, an ensemble is  
20 a collection of forecasts made from almost, but not quite, identical initial conditions.

21 A key question that arises when using a cascade modelling approach to flood prediction or  
22 mapping is: how uncertainties associated to meteorological predictions of precipitation  
23 propagate to a given flood inundation map? Previous work has been devoted to the examination  
24 of uncertainties in the results derived from different ensemble methods, which address  
25 differences in the initial conditions in the NWP or even differences in using a single model  
26 ensemble vs. multi-model ensemble (Pappenberger et al. 2008; Cloke et al., 2013; Ye et al.,  
27 2014). However, less attention has been paid to the behaviour of errors within a model chain  
28 that aims to represent a flood event occurring at several spatial scales. In order to understand  
29 how errors propagate in a chain of models, this investigation evaluates the transmission of  
30 uncertainties from the meteorological model to a given flood map. For this, we utilize a cascade  
31 modelling approach comprised by a Numerical Weather Prediction Model (NWP), a rainfall-  
32 runoff model and a standard 2D hydrodynamic model. ~~The~~ This numerical framework is applied



1 to an observed extreme event registered in Mexico in 2009 for which satellite imagery is  
2 available. The investigated uncertainty is limited to the model parameter definition in the NWP  
3 model, by means of a multi-physics ensemble technique considering several multi-physics  
4 parameterization schemes for the precipitation (Bukovsky and Karoly, 2009). The resulting  
5 precipitation fields are used to generate spaghetti plots by means of a distributed hydrological  
6 model, enabling the propagation of meteorological uncertainties to the runoff-flood hydrograph.  
7 Hence, the resulting hydrographs represent the runoff associated to each precipitation field  
8 estimated with the NWP. In order to complete the propagation of the uncertainty through  
9 the cascade of models to the flood map, the hydrographs are used as forcing in a standard 2D  
10 hydrodynamic model.

11 On the other hand, it is acknowledged that each of the other models (hydrological and  
12 hydrodynamic) within the model cascade, will introduce other epistemic and random  
13 uncertainties to the result. In order to reduce their influence, the numerical setup of both these  
14 models is constructed with the best available data (e.g. LiDAR for the topography) and  
15 following recent guidelines for the assessment of uncertainty in flood risk mapping (Beven et  
16 al. 2011). In this way, the uncertainty associated to the meteorological model outputs is  
17 propagated through the model cascade from the atmosphere to the flood plain. Thus, the aim of  
18 this investigation is to study the uncertainty propagation from the meteorological model (due  
19 to model parameters), to the determination of an affected area impacted by a well-documented  
20 hydro-meteorological event.

21 This work is organised as follows: Section 2 provides a description of both, the study area and  
22 the extreme hydro-meteorological event, which are employed to test our cascade modelling  
23 approach; Section 3 introduces the methodology, incorporating a brief description of the  
24 selected models setup. Additionally, we incorporate a description of the multi-physics ensemble  
25 technique used to quantify and limit the epistemic uncertainty in the NWP model. The resulting  
26 precipitation fields, hydrographs and flood maps are compared with available field data and  
27 satellite imagery for the event. In Section 4, a discussion of errors along the model cascade, is  
28 also presented with some conclusions and future work.

29

## 30 **2 Case Study**

31 The selected study area is within the Mexican state of Tabasco, which in recent years has been  
32 subjected to severe flooding as reported by Pedrozo-Acuña et al. (2011; 2012). This region

1 comprises the area of Mexico with the highest precipitation rate (2000-3000 mm/year), which  
2 mostly occurs during the wet season of the year between May and December. The rainfall  
3 climatology is also influenced by the incidence of hurricanes and tropical storms arriving from  
4 the North.

5 In this paper, the extreme hydro-meteorological event selected for the analysis corresponds to  
6 that registered in the early days of November 2009 in the Tonalá river. As it is shown in Fig.1,  
7 the river is located in the border of Tabasco and Veracruz and during the event, the substantial  
8 rainfall intensity provoked its overflowing leaving extensive inundated areas along its  
9 floodplain. Top panel of Fig. 1 shows the geographical location of the catchment, with an area  
10 of 5,021 km<sup>2</sup>, as well as the location of 18 weather stations installed within the region by the  
11 National Weather Service. The event was the result of heavy rain induced by the cold front #9,  
12 which persisted for four days along Mexico's Gulf Coast, forcing more than 44,000 people to  
13 evacuate their homes and affecting more than 90 communities. High intensities in rainfall were  
14 recorded in rain gauges from the 31st October to 3rd November, with cumulative daily  
15 precipitation values reporting more than 270 mm. The river is approximately 300 km long and  
16 before discharging into the Gulf of Mexico, the stream receives additional streamflow from  
17 other smaller streams such as Agua Dulcita in Veracruz, and Chicozapote in Tabasco. The  
18 bottom panel of the same Figure illustrates the lower Tonalá River, where severe flooding was  
19 registered as it is shown in the photographs on the right. The yellow, blue and red dots on the  
20 panel represent the location at which the photographs were taken.

21 The hydrometric data in combination with the satellite imagery for the characterisation of the  
22 affected areas, enabled an accurate investigation of the causes and consequences that generated  
23 this flood event. The high quality of the available information, allowed the application of a  
24 cascade modelling approach comprised by state-of-the-art meteorological, hydrological and  
25 hydrodynamic models. This numerical approach is utilised with the intention to carry out an  
26 assessment of the modelling framework, with particular emphasis on the propagation of the  
27 epistemic uncertainty from the meteorological model to the spatial extent of an affected area.  
28 Such investigation paves the road towards a more honest knowledge transfer to decision-  
29 makers, whom consider the reliability of the model results.

30

### 1   **3   Methodology and Results**

2   The methodology is comprised of a Numerical Weather Prediction Model (NWP), a distributed  
3   rainfall-runoff model and a standard 2D hydrodynamic model. It is anticipated that the selected  
4   modelling approach will support the advance of the understanding of the connections among  
5   scales, intensities, causative factors, and impacts of extremes. This model cascade with state-  
6   of-the-art numerical tools representing a hydrological system, enables the development of a  
7   framework by which an identification of the reliability of simulations can be undertaken. This  
8   framework is utilised to explore the propagation of epistemic uncertainties from the estimation  
9   of precipitation in the atmosphere to the identification of a flooded area. Therefore, the aim is  
10   not to reproduce an observed extreme event, but to investigate the effects of errors in rainfall  
11   prediction by a NWP on inundation areas.

12   The proposed investigation is important as uncertainties are cascaded through the modelling  
13   framework, in order to provide better understanding on how errors propagate within models  
14   working at different temporal and spatial scales. It is acknowledged that this information would  
15   enhance better flood management strategies, which would be based on the honest and  
16   transparent communication of the results produced by a modelling system constrained by  
17   intrinsic errors and uncertainties.

18

#### 19   **3.1   Meteorological model**

20   Simulated precipitation products from numerical weather prediction systems (NWPs) typically  
21   show differences in their spatial and temporal distribution. These differences can considerably  
22   influence the ability to predict hydrological responses. In this sense, in this study we utilise the  
23   advanced research core of the Weather Research and Forecasting (WRF) model Version 3.2.  
24   The WRF model is a fully compressible non-hydrostatic, primitive-equation model with  
25   multiple nesting capabilities ([Skamarock et al., 2008](#)).

26   As it is shown in [Fig. 2](#), the model setup is defined using an interactive nested domain inside  
27   the parent domain. This domain is selected in order to simulate more realistic rainfall, with the  
28   inner frame enclosing the Tonalá river catchment within a 4 km resolution. The 4 km horizontal  
29   resolution is considered good enough to compute a mesoscale cloud system associated to a cold  
30   front. It is shown that this finer grid covers the central region of Mexico, while in the vertical  
31   dimension, 28 unevenly spaced sigma levels were selected. The initial and boundary conditions

1 were created from the NCEP Global Final Analysis (FNL) with a time interval of 6 hours for  
2 the initial and boundary conditions. Each of the model simulations was reinitialised every two  
3 days at 1200 UTC, considering a total simulation time from the 27<sup>th</sup> October 2009 until the 13<sup>th</sup>  
4 November 2009.

5 Epistemic uncertainty is considered in the WRF model by means of the sensitivity of the results  
6 for precipitation, due to variations in the model setup. For this, we utilise a multi-physics  
7 ensemble technique proposed by Bukovsky and Karoly (2009), where the sensitivity of  
8 simulated precipitation in the model results is examined with twelve different parameterisation  
9 schemes. The comparison of computed precipitation fields against real measurements from  
10 weather stations within the catchment, enabled the quantification of uncertainty in the  
11 meteorological model for this event. **Table 1** shows a summary of the different multi-physics  
12 parameters used in the WRF model to generate the physics ensemble. In this approach, the  
13 multi-physics ensemble runs of the model represent a plausible and equally likely state of the  
14 system in the future.

15 **Fig. 3** illustrates the cumulative precipitation fields computed for each of the 12 selected  
16 members of the multi-physics ensemble, where differences in the spatial distribution and  
17 intensity of precipitation were evident. These results suggested that for this event, the  
18 precipitation field estimated with the WRF was highly sensitive to the selection of multi-physics  
19 parameters. To revise in more detail the performance of the WRF in reproducing this hydro-  
20 meteorological event, the estimated cumulative precipitation by each member of the multi-  
21 physics ensemble was compared against measurements at the eighteen weather stations located  
22 within and close to the Tonalá catchment.

23 **Table 2** presents a summary of the most well-known error metrics calculated at each weather  
24 station and for each member of the ensemble. Among these are the: Normalised Root-Mean  
25 Square Error (NRMSE), BIAS, Nash-Sutcliffe Coefficient (NSC), and the Correlation  
26 coefficient (Cor). The columns show the local value of each coefficient for a given member of  
27 the ensemble (M1, ..., M12). As shown in all columns (i.e. member runs), the error metrics  
28 have a great spatial variability, hence, indicating the regions of the study area where the model  
29 performs better. To illustrate the performance of this ensemble technique at each weather  
30 station, the ensemble average of these error metrics ~~are~~ introduced in the last column and  
31 indicated by < >. Again, the spatial variability of the metrics is evident. The two bottom rows  
32 in each sub-table correspond to the average of the ensemble averages for the whole catchment

1 and for the all the stations. It is shown, that when the average of all stations is taken into account,  
2 the skill decreases. However, in this investigation the error that is of interest is the one  
3 corresponding to the average of those weather stations located within the catchment, as these  
4 will be used as input in the hydrological model. This will enable the propagation of errors in  
5 the meteorological model within the model cascade. For clarity, in the same table the stations  
6 within the catchment are highlighted in blue.

7 Additionally, results per station are also illustrated for four different cases and are presented in  
8 **Fig. 4**, and they confirmed that the range of spatial uncertainty in the WRF predictions is high  
9 and variable. To give an example, at Station No. 27075, the spread of the estimated cumulative  
10 precipitation curves is limited and quantified by a NSC=0.917 and a NRMSE = 10.7%,  
11 indicating a good skill of the WRF precipitation estimates at this point. In contrast, at Station  
12 No. 27007 the spread of the cumulative precipitation is large and characterised by a NSC=0.766  
13 and a NRMSE=19.4%, showing less skill in the model performance than that observed in the  
14 previous case. The observed differences of estimated precipitation for this event, highlight the  
15 importance of incorporating ensemble techniques in the reproduction of precipitation with this  
16 type of models.

17 A question that has been seldom explored in the literature, is how the uncertainty in the  
18 prediction of the precipitation (i.e. errors described in this section), cascade into an estimated  
19 flood hydrograph determined by a distributed hydrological model. In this sense, the next step  
20 in this work, considers the non-linear transfer of rainfall to runoff using a distributed rainfall-  
21 runoff model. For this, we employ each one of the 12 precipitation fields derived from the WRF  
22 as input to determine the associated river discharge with the hydrological model.

23

## 24 **3.2 Hydrological model**

25 The hydrological model used in this study was applied to the Tonalá River catchment in an  
26 early work presented by [Rodríguez-Rincón et al. \(2012\)](#). This numerical tool was developed by  
27 the Institute of Engineering – UNAM ([Domínguez-Mora et al., 2008](#)), and comprises a  
28 simplified grid-based distributed rainfall–runoff model. The model has been previously applied  
29 with success in other catchments in Mexico (e.g. [Pedrozo-Acuña et al., 2014, 2014b](#)).

30 ~~This paper only describes an overview and key components of the hydrologic model. Interested~~  
31 ~~readers can find detailed descriptions in Domínguez-Mora et al. (2008).~~ The model is based on

1 the method of the Soil Conservation Service (SCS) with a modification that allows the  
 2 consideration of soil moisture accounting before and after rainfall events. The parameters that  
 3 are needed for the definition of a runoff curve number within the catchment are the hydrological  
 4 soil group, land use, pedology and the river drainage network. **Fig. 5** shows for the Tonalá  
 5 River catchment, the spatial definition of the river network (center panels) and the runoff curve  
 6 (right panels). ~~The model is forced with the precipitation calculated from~~ For the WRF  
 7 considering the 12 members numerical setup of the multi-physics ensemble hydrological model,  
 8 we employ topographic information from a LiDAR data set, from which a 10m resolution  
 9 Digital Elevation Model (DEM) is constructed.

10 There are two main hypothesis that underpin the SCS curve number method. Firstly, it is  
 11 assumed that for a single storm and after the start of the runoff, the ratio between actual soil  
 12 retention and its maximum retention potential is equal to the ratio between direct runoff and  
 13 available rainfall. Secondly, the initial infiltration is hypothesised to be a fraction of the  
 14 retention potential.

15 Thus, the water balance equation and corresponding assumptions are expressed as follows:

$$16 \quad P = P_e + I_a + F_a \quad (1)$$

$$17 \quad \frac{P_e}{P_a - I_a} = \frac{F_a}{S} \quad (2)$$

$$19 \quad I_a = \lambda S \quad (3)$$

20 Where  $P$  is rainfall,  $P_e$  effective rainfall,  $I_a$  is the initial abstraction,  $F_a$  is the cumulative  
 21 abstraction,  $S$  is the potential maximum soil moisture retention after the start of the runoff and  
 22  $\lambda$  is the scale factor of initial loss. The value of  $\lambda$  is related to the maximum potential infiltration  
 23 in the basin.

24 Through the combination of equations (1) - (3) and expressing the initial abstraction ( $I_a$ ) by  
 25  $0.2*S$  we have:

$$26 \quad P_e = \frac{(P - 0.2S)^2}{P + 0.8S} \quad (4)$$

28 where, the value of  $S$  [cm] is determined by:

29

$$S = \frac{2450 - (25.4CN)}{CN} \quad (5)$$

*CN* is the runoff curve number, as defined by the Agriculture Department of the USA (USDA, 1985). Values for this parameter vary from 30 to 100, where small numbers indicate low runoff potential while larger numbers indicate an increase in runoff potential. Thus, the permeability of the soil is inversely proportional to the selected curve number. Another parameter that allows the modification of the curve number is the soil water potential given by *F<sub>s</sub>*, following  $S=S*F_s$ . The model includes a parameter to reproduce the effects of evaporation on the ground saturation (*F<sub>o</sub>*). This parameter is useful when the event to be reproduced lasts for several days; however, due to the duration of this event it is assumed equal to 0.9 in all cases. The computation of the runoff in the basin is carried out through the addition of the runoff estimated in each cell to then construct a general hydrograph (See Rodríguez-Rincón et al. 2012). With regards to the definition of values for the other two free parameters in the hydrological model ( $\lambda$  and *F<sub>s</sub>*), a traditional calibration process is implemented. For this, we utilise flood hydrographs from past extreme events (2001, 2005, 2007, 2008, 2009 and 2011) observed in this river. Therefore, we determine six sets of free parameters that are good enough to represent the rainfall-runoff relationship in this catchment. The selected sets of values are illustrated in **Table 3**, where the correlation coefficient and NSC are also reported for each of the years. It is shown that in all the events, the selected set of parameters ensures a good correlation against the observed discharge which is given by  $Cor > 0.7$ , as well as a positive NSC (accuracy).

It is well known that both the amount and distribution of rainfall can significantly affect the final estimated river discharge (Ferraris et al. 2002; De Roo et al., 2003; Cluckie et al., 2004). In consequence, the propagation of meteorological uncertainty to the rainfall-runoff model is carried out using the 12 WRF rainfall precipitation ensembles as an input in the hydrological model. For this purpose, considering the six sets of free-parameters reported in the hydrologic model are fixed, assuming **Table 3**. This procedure enabled the generation of 72 hydrographs that the selected parameters are the best at representing could represent the physical conditions of the catchment for this 2009 event. The selection of these parameters is carried out following the results presented by Rodríguez-Rincón et al. (2012) for the same catchment. For the numerical setup of the hydrological model, we employ topographic information from a LiDAR data set, from which a 10m resolution Digital Elevation Model (DEM) is constructed. with different skill. Error metrics of all the computed hydrographs are reported in **Table 4**.

1 For completeness, Fig. 6a illustrates the 72 computed hydrographs for the Tonalá River  
2 catchment the spaghetti plot of hydrographs computed in relation to the measured river  
3 discharge for this the 2009 event, these are (blue dashed line). It is shown that if all 72  
4 hydrographs are taken into account, uncertainty bounds are significant. Indeed, this illustrates  
5 the interaction of the meteorological uncertainty with that coming from the setup of the  
6 hydrological model (definition of free parameters). However, the purpose of this study is to  
7 investigate in a model cascade framework, how errors in the meteorological prediction stage  
8 propagate down to a predicted inundation. In this sense, we narrow down the number of  
9 hydrographs shown in Fig. 6a, by selecting only those with a  $Cor > 0.7$  and  $NSC > 0.6$ , as  
10 reported in Table 4 only 31 out of 72 (shown in bold) follow this condition. Fig. 6b displays  
11 the 31 selected hydrographs along with the measured discharge by for the 2009 event. Although  
12 there is a streamflow gauge. The reduction in the uncertainty bounds illustrated by the grey  
13 shaded area indicate, it is shown that errors in the predicted rainfall are indeed propagated to  
14 the hydrological model, which uses employs a finer spatial resolution (1 km). It has been  
15 established that, in some cases, an error in the meteorological model can be compensated by an  
16 error in the hydrological model and vice-versa. To illustrate this in more detail, Table 3 presents  
17 a summary average values of the calculated error metrics for the 31 selected hydrographs shown  
18 in Fig. 6. It is shown that on average (last column are estimated and reported in Table 4, with  
19  $NSC = 0.79$ ,  $Cor = 0.96$  and  $BIAS = 1.11$ . Values of the NSC for selected hydrographs in the  
20 Table) 4 illustrate the resulting differences in skill resulting from the combination of different  
21 setups in the hydrological model has a  $NSC = 0.84$ ,  $Cor = 0.96$ ,  $BIAS = 1.01$  and  
22  $NRMSE = 38.12\%$ . Differences between members of the with the multi-physics ensemble are  
23 also illustrated at this stage, especially by the NSC. For instance, in the rows corresponding to  
24 the parametes determined for the 2011 event, member M11M12 indicates a  $NSC = 0.68738$   
25 showing ~~poora~~ poorer skill at reproducing the river discharge with the precipitation derived  
26 from this member, in contrast comparison to that registered for member M3 has a greater  
27 skillM2 with  $NSC = 0.93938$ . The change in the values of the NSC indicates that results from  
28 the regional weather model can be enhanced or weakened by the performance of the  
29 hydrological model.

30 The useutilisation of these the 31 selected hydrographs in a 2D hydrodynamic model, enables  
31 the study of the propagation of errors within the cascade of models. In particular, for estimating  
32 the flood extent during this extreme event.



1

### 2 3.3 Flood inundation model

3 Several 2D hydrodynamic models have been developed for simulating extreme flood events.  
4 However, any model is only as good as the data used to parameterise, calibrate and validate the  
5 model. 2D models have been regarded as suitable for simulating problems where inundation  
6 extent changes dynamically through time as they can easily represent moving boundary effects  
7 (e.g. [Bates and Horritt, 2005](#)). The use of these numerical tools has become common place  
8 when flows produce a large areal extent, compared to their depth and where there are large  
9 lateral variations in the velocity field ([Hunter et al., 2008](#)).

10 In this study, given the size of the study area the modelling system utilised is comprised by the  
11 flow model of MIKE 21 flexible mesh (FM). This numerical model solves the two dimensional  
12 Reynolds-averaged Navier–Stokes equations invoking the approximations of Boussinesq and  
13 hydrostatic pressure. ~~This involves continuity, momentum, temperature, salinity and density~~  
14 ~~equations~~ (for details see [DHI, 2014](#)). The equations are solved at the centre of each element in  
15 the model domain.

16 The numerical setup is based on a previous work on the study area ([Pedrozo-Acuña et al. 2012](#)),  
17 with selected resolutions for the elements of the mesh with a size that guarantees the proper  
18 assimilation of a 10 m DEM to characterise the elevation in the floodplain. The topographic  
19 data has been regarded as the most important factor in determining water surface elevations,  
20 base flood elevation, and the extent of flooding and, thus, the accuracy of flood maps in riverine  
21 areas ([NRC, 2009](#)). Therefore, the elevation data used in this study corresponds to LiDAR data  
22 ~~provided by INEGI (2008). The hydraulic roughness in the floodplain is assumed to be uniform~~  
23 ~~and different from the main river channel, in this sense two values for the Manning number are~~  
24 ~~used, one for the main river channel ( $M=32 \text{ m}^{1/2}\text{s}^{-1}$ ) and another for the floodplain ( $M=28 \text{ m}^{1/2}\text{s}^{-1}$ ).~~  
25 ~~set provided by INEGI (2008).~~ The choice of a 10-m DEM is based on recommendations  
26 put forward by the Committee on Floodplain Mapping Technologies, [NRC \(2007\)](#) and [Prinos](#)  
27 [et al. \(2008\)](#), as such a DEM ensures both accuracy and detail of the ground surface. The model  
28 domain is illustrated in [Fig. 7](#), along with the numerical mesh and elevation data, it comprises  
29 the lower basin of the Tonalá River and additional main water bodies. The colours represent  
30 the magnitude of the elevation and bathymetric data assimilated in the numerical mesh, where  
31 warm colours identify high ground areas and light blues represent bathymetric data. ~~The~~

1 ~~numerical mesh considers three boundary conditions represented in the Figure by dots as~~  
2 ~~follows: where the input hydrograph from the rainfall-runoff model is set (red dot); the Tonalá's~~  
3 ~~river mouth, where the astronomical tide for the period of the event (27<sup>th</sup> October – 12<sup>th</sup>~~  
4 ~~November 2009) (yellow dot) and the Agua Dulcita river set where a constant discharge of~~  
5 ~~100 m<sup>3</sup>/s is introduced (blue dot).~~

6 ~~It is acknowledged that topographic information is key for the reduction of uncertainty in flood~~  
7 ~~hazard mapping. Therefore, in order to minimise this source of error, the~~The ~~integration of high~~  
8 ~~quality topographic information in a 2D model with enough spatial resolution, will~~  
9 ~~enable~~enables ~~the investigation of the propagation of the meteorological uncertainty to the~~  
10 ~~determination of the flood extent. Moreover, as it is illustrated in Fig. 7 the numerical mesh~~  
11 ~~considers three boundary conditions. These are input flow boundary where the hydrograph from~~  
12 ~~the rainfall-runoff model is set (red dot); the Tonalá's river mouth, where the astronomical tide~~  
13 ~~occurs for the period of the event (27<sup>th</sup> October – 12<sup>th</sup> November 2009) (yellow dot) and the~~  
14 ~~Agua Dulcita river set where a constant discharge of 100 m<sup>3</sup>/s is introduced (blue dot).~~

15 ~~On the other hand, hydraulic roughness is a lumped term known as Manning's coefficient that~~  
16 ~~represents the sum of a number of effects, among which are skin friction, form drag and the~~  
17 ~~impact of acceleration and deceleration of the flow. The precise effects represented by the~~  
18 ~~friction coefficient for a particular model depend on the model's dimensionality, as the~~  
19 ~~parameterisation compensates for energy losses due to unrepresented processes, and the grid~~  
20 ~~resolution (Bates et al., 2014). The lack of a comprehensive theory of "effective roughness"~~  
21 ~~have determined the need for calibration of friction parameters in hydraulic models.~~  
22 ~~Furthermore, the determination of realistic spatial distributions of friction across a floodplain~~  
23 ~~in other studies, have showed that only 1 or 2 floodplain roughness classes are required to match~~  
24 ~~current data sources (Werner et al., 2005). Indeed, this suggests that application of complex~~  
25 ~~formulae to establish roughness values for changed floodplain land use are inappropriate until~~  
26 ~~model validation data are improved significantly. Therefore, in this study hydraulic roughness~~  
27 ~~in the floodplain is assumed to be uniform and different from the main river channel, in this~~  
28 ~~sense two values for the Manning number are used, one for the main river channel ( $M=32 \text{ m}^{1/2}\text{s}^{-1}$ )~~  
29 ~~and another for the floodplain ( $M=28 \text{ m}^{1/2}\text{s}^{-1}$ ).~~

30 ~~In order to assess whether the 2D model is able to reproduce the flood extent observed in 2009,~~  
31 ~~numerical results of flood extent are compared against the affected area determined from a~~  
32 ~~SPOT image (resolution of 124m). This practice is widely used in the literature to evaluate the~~

1 results from inundation models and to compare its performance (Di Baldassare et al, 2010b;  
2 Wright et al., 2008).

3 **Fig. 8a** introduces the result of the hydrodynamic simulation for each of the 4231 selected  
4 hydrographs, which resulted from the utilisation of the rainfall-runoff model using as input the  
5 WRF multi-physics ensemble output. The illustrated flood map summarises the 4231 different  
6 possibilities of the inundation area that could result from the characterisation of precipitation  
7 with the WRF model. ~~Differences in the size of these areas, illustrate the propagation of~~  
8 ~~epistemic errors from the meteorological model to the flood map. In this sense, the analysis of~~  
9 ~~uncertainty has been restricted to its propagation along the model chain (atmosphere-~~  
10 ~~catchment-river floodplain).~~ Each of these flood maps can also be associated to a probability  
11 enabling the representation of a probabilistic flood map, shown in the figure. This allows the  
12 identification of the areas highly vulnerable to flooding from this event. Additionally, **Fig. 8b**  
13 introduces the infrared SPOT satellite image of the 12<sup>th</sup> of November 2009, which is used for  
14 comparison against the produced flood maps ~~using all the ensemble members derived from~~  
15 ~~running the 31 hydrographs as inputs in the 2D model~~. Notably, in the numerical results, the  
16 blue area identifies the region of the domain that is most likely to be flooded (90%), the  
17 comparison of this area with the observed inundation in the satellite image, show a good skill  
18 of the model chain at reproducing the registered flood in the study area.

19 ~~To better quantify the performance of each of the model runs in reproducing the observed flood~~  
20 ~~extent, the estimation of several error metrics in these results was also performed, among these~~  
21 ~~are~~ Despite the variability in the estimated peak discharge utilised as input in the different  
22 hydrodynamic runs, inundation results show similar affected areas in all realisations (only with  
23 small differences in its size). This is verified in the results shown in **Fig. 9a**, where the  
24 relationship between peak discharge of the 31 hydrographs, is plotted against the size of the  
25 maximum-flooded area. The distribution of points in this graph clearly indicates that although  
26 there are differences in the estimated peak flow (see histogram in Fig. 9b), in most cases the  
27 resulting size of the inundated area is similar. Histogram plot shown in **Fig. 9c** indicates a clear  
28 concentration numerically derived flooded areas with a size larger than 130 km<sup>2</sup>. Indeed, the  
29 mean value of the maximum-flooded estimated area is 138.94 km<sup>2</sup>, while the standard deviation  
30 is 16.09 km<sup>2</sup>.

31 These results support that the hydraulic behaviour in all hydrodynamic simulations was indeed  
32 very similar, regardless of the peak discharge of the hydrograph. It is reflected that this may be

1 the result of induced hydrodynamics by a valley-filling flood event, which is identified with the  
2 relatively high floodplain area-to-channel-depth ratios in all simulations. Hence, all possible  
3 hydrographs generated with the hydrological model show similar levels of lateral momentum  
4 exchange between main channel and floodplain. For this reason, the predictive performance of  
5 all hydrodynamic simulations used to reproduce the inundation extent appears to be good (see  
6 Table 5).

7 The estimation of several error metrics in these results was performed using binary flood extent  
8 maps, where the comparison is based on the generation of a contingency table, which reports  
9 the number of pixels correctly predicted as wet or dry. From this, measures of fit such as: BIAS,  
10 False Alarm Ratio (FAR), Probability of Detection (POD), Probability of False Detection  
11 (POFD), Critical Success Index (CSI) and the True Skill Statistics (TSS) are estimated. Table  
12 45 introduces the results by member for all 31 members and metric error metrics. Clearly, there  
13 is some little variability in the performance of the model for each of the ensemble members runs,  
14 showing that there has been some a small propagation of the error to the flood map. The  
15 ensemble average of these quantities is also illustrated in the last column of the table, where  
16 a values of BIAS=0.9641,013, FAR=0.453189, POD=0.799819, POFD=0.154180;  
17 CSI=0.834686 and TSS=0.645639 are reported. These As noted before, these results indicate  
18 an apparent good skill of the model chain at reproducing the flood extension, due to the  
19 incidence of this extreme event. It should be borne in mind, however, that some  
20 misclassification errors may also be included in the observed flooded area due to specular  
21 reflections that may classify some wet vegetation as water or open water as dry land. In  
22 consequence, flood extent maps should be used with caution in assessing model performance  
23 (Di Baldassare, 2012). This is particularly true during high-magnitude events where the valley  
24 is entirely inundated, such as the case study of this investigation where small changes in lateral  
25 flood extent may produce large changes in water levels.

26 In this sense, it has been argued that flood extent maps are not useful for model assessment  
27 (Hunter et al., 2005) and high water marks are more useful to evaluate model performance.  
28 Unfortunately, for the case study information of inundation depths was not available. Despite  
29 this fact, a further revision of simulated inundation depths is also carried out. For this, 10 points  
30 distributed within the numerical domain are selected. These are illustrated by the coloured dots  
31 in Fig. 10, along with the values of mean water depth in all the 31 simulations (red solid line).  
32 In all cases, a high variability in the estimated inundation depth on the floodplain is depicted

1 (with values varying between 1.5 and 3m). This result supports that in the case of valley-filling  
2 flood events, there is a higher sensitivity to errors in the vertical dimension of the flood.

3 In one hand, this demonstrates that the geomorphological characteristics of the site (e.g. low-  
4 lying area, smooth slopes in the river channel and floodplain) are dominant in the accurate  
5 determination of the magnitude of an inundated area, regardless of the peak discharge. This  
6 implies that for this type of rivers and when predicting inundation extent, it may be more  
7 important to have a good characterisation of the river and floodplain (e.g. high quality field data  
8 and a LiDAR derived DEM), than a good characterisation of the rainfall-runoff relationship.

9 Current approaches to flood mapping, have pointed out that in order to produce a scientifically  
10 justifiable flood map, the most physically-realistic model should be utilised (Di Baldassarre et  
11 al., 2010). Nevertheless, even with these models the amount of uncertainty involved in the  
12 determination of an affected area is important and should be quantified.

#### 14 **4 Discussion and Conclusions**

15 ~~It has been largely acknowledged in the literature, that flood~~Flood risk mapping and assessment  
16 are highly difficult tasks due to the inherent complexity of the relevant processes, which occur  
17 in several spatial and temporal scales. As pointed out by Aronica et al. (2013), the ~~process~~  
18 ~~is~~processes are subject to substantial uncertainties (epistemic and random), which emerge from  
19 different sources and ~~idealisation of processes~~assumptions, from the statistical analysis of  
20 extreme events and from the resolution and accuracy of the DEM used in a flood inundation  
21 model.

22 By acknowledging that all models are an imperfect representation of the reality, it is important  
23 to quantify the impact of epistemic uncertainties on a given result. The numerical approach  
24 utilised in this investigation enabled an assessment of a state-of-the art modelling framework,  
25 comprised by meteorological, hydrological and hydrodynamic models. Emphasis was given to  
26 the effects of epistemic uncertainty propagation from the meteorological model to the definition  
27 of an affected area in a 2D domain. Ensemble climate simulations have become a common  
28 practice in order to provide a metric of the uncertainty associated with climate predictions. In  
29 this study, a multi-physics ensemble technique is utilised to evaluate the propagation of  
30 epistemic uncertainties within a model chain. Therefore, the assessment of hydro-

1 meteorological model performance at the three stages is carried out through the estimation of  
2 skill scores.

3 **Fig. 911** presents a summary of the propagation of two well-known error metrics, BIAS (top  
4 panel) and NSC/TSS (bottom panel). These metrics ~~are~~were selected, as they enable a direct  
5 comparison of their values at each of the stages within the model cascade. In both metrics, the  
6 evolution of the confidence limits is illustrated by the size of the bars. Their evolution from the  
7 meteorological model to the hydrological model ~~results, show a clear decrease in both cases.~~  
8 ~~This result may point towards~~, show an enhancementaggregation of meteorological  
9 uncertainties ~~in~~with those originated from the rainfall-runoff model. However, the skill ~~of the~~  
10 ~~hydrological model~~ is considerably improved from a mean value of 0.65 in the meteorological  
11 model, to 0.834793 in the hydrological model. In the last stage of the model chain,  
12 (hydrodynamic model), the confidence limits of the results ~~at the hydrodynamic model results,~~  
13 show a smallan apparent improvement. ~~Nevertheless, in model skill. However, it should be~~  
14 noted that this may be ascribed to the complex aggregation of errors in valley-filling events,  
15 which is verified in the observed sensitivity of the simulated inundation depths. The mean value  
16 of the skill is reduced to TSS=0.645639. The results provide aan useful way to evaluate the  
17 hydro-meteorological uncertainty propagation within the ~~whole hydro-meteorological~~  
18 modelling cascade system.

19 BIAS and NSC/TSS error metrics (Fig. 11) revealed discrepancies between observations and  
20 simulations throughout the model cascade. For instance, an increase in the NSC from the  
21 rainfall to the flood hydrograph it implies that the hydrological model is more sensitive (wider  
22 uncertainty bars) to its main input (precipitation) than the WRF model is to the set of micro-  
23 physics parameterisations. On the other side, the uncertainty bounds in the hydrological model  
24 imply a high sensitivity of hydrographs to both, errors from the meteorological model and its  
25 numerical setup with free parameters (amplifying the uncertainty). This is observed in the  
26 spaghetti plot shown in Fig. 6a, where large uncertainty bounds were identified. In order to  
27 reduce errors from the interaction of uncertainties coming from both models, these bounds were  
28 reduced with the selection of 31 hydrographs that comply with  $Cor > 0.7$  and  $NSC > 0.6$  (see  
29 Fig.6b). It is reflected that the estimated error in the meteorological model may reflect a spatial  
30 scaling issue (comparing observations from rain gauges to simulations at the meso-scale).

31 Results concerning predictions of inundation extent indicate an apparent good skill of the model  
32 chain at reproducing the flood extension. The propagation of uncertainty and error from the

1 hydrological model to the inundation area revealed that is necessary to assess model  
2 performance not only for flood extension purposes, but also to estimate inundation depths,  
3 where results indicate a higher variability (e.g. increase in the error). This last modelling step  
4 is quite important given the consequences for issuing warning alerts to the population at risk.

5 The similar magnitude in inundation extents of all numerical results indicated the predominance  
6 of a valley-filling flood event, which was characterised by a flooded area strongly insensitive  
7 to the input flood hydrograph. While this can be explained by the limited effect that the volume  
8 overflowing the riverbanks and reaching the floodplain will have on the maximum inundation  
9 area, the difference between the observed and the simulated flooded area remains important  
10 (TSS=0.639).

11 It should be pointed out, that this methodology contains more uncertainties that were not  
12 considered or quantified in the generation of flood extent maps for this event. To quantify the  
13 epistemic uncertainty in the larger scale (i.e. atmosphere), a mesoscale numerical weather  
14 prediction system was used along with a multi-physics ensemble. The ensemble was designed  
15 to represent our limited knowledge of the processes generating precipitation in the  
16 meteorological system. The propagation of this uncertainty to a rainfall-runoff model revealed  
17 large spatial variations of the model skill across scales and models. lower troposphere. It was  
18 shown that a large amount of uncertainty exists in the NWP model, and this such uncertainty is  
19 indeed propagated over the catchment and floodplain scales. Members of the ensemble were  
20 shown to differ significantly in terms of their cumulative precipitation, its spatial distribution,  
21 river discharge and the size of the affected area by the event., inundation depths and areas.  
22 Therefore, epistemic uncertainties from each step in the hazard analysis chain accumulate in  
23 this model cascade can be aggregated up to the final outputs/output.

24 The evaluation of the skill in the model cascade shows further potential for improvements of  
25 the model/modelling system. Consequently, future work is planned to include the remaining  
26 uncertainties as adopted by, e.g. [Pedrozo-Acuña et al. \(2013\)](#). Special attention should be paid  
27 to the interaction of-between hydro-meteorological and hydrological uncertainty, as well as  
28 flood extent estimation in catchments with that of hydrological origin/different morphological  
29 setting. The assessment of the error propagation within the model cascade is seen as a good step  
30 forward, in the communication of uncertain results to the society. The/However, as shown in  
31 this work, an improvement in model prediction during the first cascade step (rainfall to runoff)  
32 can be reverted during the second cascade step (runoff to inundation area) with important

1 consequences for early warning systems and operational forecasting purposes. Finally, the  
2 proposed numerical framework could be utilised as a robust alternative for the characterisation  
3 of extreme events in ungauged basins.

4 ~~The acknowledgment of these uncertainties, by showing their impact on model results, favour~~  
5 ~~preventive action in the production of methodologies that evaluate flood extension with some~~  
6 ~~level of confidence. Therefore, the investigation paves the road towards a more honest~~  
7 ~~knowledge transfer to decision-makers, whom consider the reliability of the model results.~~

## 10 **Acknowledgements**

11 The authors thank the financial support from the Institute of Engineering, UNAM, through  
12 internal and international grants. The authors gratefully acknowledge the comments and  
13 suggestions made by two anonymous referees and Prof. Jim Freer, handling editor of this  
14 manuscript.

## 16 **References**

17 Aronica, G. T., Apel, H., Baldassarre, G. D. and Schumann, G. J.-P. 2013. HP – Special Issue  
18 on Flood Risk and Uncertainty. *Hydrol. Process.*, 27: 1291. doi: 10.1002/hyp.9812

19 Bartholmes, J., Todini, E. 2005. Coupling meteorological and hydrological models for flood  
20 forecasting, *Hydrol. Earth Syst. Sci.*, 9, 333-346, doi:10.5194/hess-9-333-2005.

21 Bartholmes, J., Thielen, J., Ramos, M., Gentilini, S., 2009. The European flood alert system  
22 EFAS – Part 2: statistical skill assessment of probabilistic and deterministic operational  
23 forecasts. *Hydrology and Earth System Sciences*, 2: 141–153.

24 Bates, P.D., Horritt, M.S. 2005. Modelling wetting and drying processes in hydraulic models.  
25 In Bates, P.D., Lane, S.N. and Ferguson, R.I. (eds), *Computational Fluid Dynamics:*  
26 *applications in environmental Hydraulics*, John Wiley and Sons, Chichester, UK

27 Bates, P.D., Pappenberger, F., Romanowicz, R.J. 2014. Uncertainty in Flood Inundation  
28 Modelling. In Beven, K.J., and Hall, J. (eds.), Applied Uncertainty Analysis for Flood Risk  
29 Management, Imperial College Press, World Scientific, London, UK

30 Becker, A. & Grünewald, U. 2003. Flood risk in central Europe. *Science* 300, 1099.



- 1 Beven, K.J. 2011. I believe in climate change but how precautionary do we need to be in  
2 planning for the future? *Hydrological Processes* 25: 1517–1520.
- 3 Beven, K.J. 2014. Use of Models in Flood Risk Management. In Beven, K.J., and Hall, J. (eds.),  
4 *Applied Uncertainty Analysis for Flood Risk Management*, Imperial College Press, World  
5 Scientific, London, UK
- 6 Beven, K., Leedal, D., McCarthy, S., Lamb, R., Hunter, N., Keef, C., Bates, P., Neal, J. and  
7 Wicks, J. 2011. Framework for Assessing Uncertainty in Fluvial Flood Risk Mapping. FRMRC  
8 Research Report SWP1.7
- 9 Buizza R. 2008. The value of probabilistic prediction. *Atmospheric Science Letters*, 9: 36–42.
- 10 Bukovsky, M. S. and D. J. Karoly. 2009. Precipitation simulations using WRF as a nested  
11 regional climate model. *Journal of Applied Meteorology and Climatology*, 48(10): 2152-2159.
- 12 Cloke, H. L. and Pappenberger, F. (2008). Evaluating forecasts for extreme events for  
13 hydrological applications: an approach for screening unfamiliar performance measures,  
14 *Meteorol. Appl.*, 15(1), 181–197.
- 15 Cloke, H.L., Pappenberger, F. 2009. Ensemble flood forecasting: A review. *Journal of*  
16 *Hydrology*, doi:10.1016/j.jhydrol.2009.06.005
- 17 Cloke, H. L., Wetterhall, F., He, Y., Freer, J. E. and Pappenberger, F. 2013. Modelling climate  
18 impact on floods with ensemble climate projections. *Q.J.R. Meteorol. Soc.*, 139: 282–297. doi:  
19 10.1002/qj.1998
- 20 Cluckie I., Han D., Xuan Y. 2004. Preliminary Analysis on NWP-Based QPF over UK domain.  
21 Deliverable 4.2, FLOODRELIEF Project, URL: <http://projects.dhi.dk/floodrelief/>
- 22 Committee on Floodplain Mapping Technologies, NRC. 2007. Elevation data for floodplain  
23 mapping. Washington, DC: National Academic Press.
- 24 Committee on FEMA Flood Maps; Board on Earth Sciences and Resources/Mapping Science  
25 Committee; NRC. 2009. Mapping the Zone: Improving Flood Map Accuracy. Washington, DC:  
26 National Academic Press.
- 27 CONAGUA. *Atlas digital del Agua México 2010*, Sistema Nacional de Información del Agua  
28 (2010). <ftp://ftp.conagua.gob.mx/>.

- 1 Cuo, L., T. C. Pagano, and Q. J. Wang, 2011: A review of quantitative precipitation forecasts  
2 and their use in short to medium range streamflow forecasting. *J. Hydrometeor.*, 12, 713–728,  
3 doi:10.1175/2011JHM1347.1.
- 4 Demeritt, D., Nobert, S., Cloke, H., and Pappenberger, F. 2010. Challenges in communicating  
5 and 5 using ensembles in operational flood forecasting, *Meteorol. Appl.*, 17, 209–222.
- 6 De Roo A., Gouweleeuw B., Thielen J., Bartholmes J. et al. 2003. Development of a European  
7 flood forecasting system. *International Journal of River Basin Management* 1(1): 49–59
- 8 DHI. MIKE 21 FM Flow model, Scientific documentation. 2014, DHI Group, Horslhome
- 9 Di Baldassarre G. 2012. *Floods in a Changing Climate: Inundation Modelling*. *International*  
10 *Hydrology Series*, Cambridge University Press, Online ISBN:9781139088411, doi:  
11 <http://dx.doi.org/10.1017/CBO9781139088411>
- 12 Di Baldassarre G., Schumann G., Bates P.D., Freer J.E., Beven K.J. 2010. Floodplain mapping:  
13 a critical discussion of deterministic and probabilistic approaches, *Hydrological Sciences*  
14 *Journal*, 55:3, 364-376, doi: 10.1080/02626661003683389.
- 15 Di Baldassarre, G., Montanari, A., Lins, H., et al. 2010b. Flood fatalities in Africa: from  
16 diagnosis to mitigation. *Geophysical Research Letters*, 37, L22402,  
17 doi:10.1029/2010GL045467
- 18 Domínguez M. R., Esquivel G. G., Méndez A. B., Mendoza R. A., Arganis J. M. L., Carrizosa  
19 E. E., 2008. Manual del Modelo para pronóstico de escurrimiento. Instituto de Ingeniería.  
20 Universidad Nacional Autónoma de México. ISBN 978-607-2-00316-3.
- 21 Ferraris L., Rudari R., Siccardi F. 2002. The uncertainty in the prediction of flash floods in the  
22 Northern Mediterranean environment. *Journal of Hydrometeorology* 3: 714–727
- 23 Fowler HJ, Blenkinsop S, Tebaldi C. 2007a. Linking climate change modelling to impacts  
24 studies: recent advances in downscaling techniques for hydrological modelling. *International*  
25 *Journal of Climatology* 27: 1547–1578.
- 26 Giorgi, F. 1990. Simulation of regional climate using a limited area model nested in a general  
27 circulation model, *J. Clim.*, 3, 941– 963.
- 28 Giorgi, F. 2006. Regional climate modeling: Status and perspectives, *J. Phys. IV*, 139, 101–  
29 118.

1 Hacking, I. 2006 The emergence of probability, 2nd edn. New York, NY: Cambridge University  
2 Press.

3 Horritt M.S., Bates P.D. 2002. Evaluation of one-dimensional and two-dimensional models for  
4 predicting river flood inundation. *Journal of Hydrology* 268: 87–99.

5 Horritt M.S., Bates P.D., Mattinson M.J. 2006. Effects of mesh resolution and topographic  
6 representation in 2D finite volume models of shallow water fluvial flow. *Journal of Hydrology*  
7 329: 306–314. DOI:10.1016/j.jhydrol.2006.02.016.

8 Hunter, [N. M., Bates, P. D., Horritt, M. S., et al. 2005. Utility of different data types for](#)  
9 [calibrating flood inundation models within a GLUE framework. \*Hydrology and Earth System\*](#)  
10 [Sciences, 9\(4\), 412–430.](#)

11 [Hunter, M., Bates, P.D., Neelz, S., Pender, G., Villanueva, I., Wright, N.G., Liang, D., Falconer,](#)  
12 [A., Lin, B., Waller, S., Crossley, A.J., Mason, D.C., 2008, Benchmarking 2D hydraulic models](#)  
13 [for urban flooding, \*Water Management\*, 161, Issue WM1, 13-30.](#)

14 INEGI. 2008. Nube de Puntos LIDAR ajustada al Terreno, Bloque conformado por las cartas  
15 1:50,000: E15A75, E15A76, E15A85, E15A86 del Instituto Nacional de Estadística, Geografía  
16 e Informática, México.

17 Jankov, I., W. A. Gallus, et al. The Impact of Different WRF Model Physical Parameterizations  
18 and Their Interactions on Warm Season MCS Rainfall. *Weather and Forecasting* 20, (2005):  
19 1048-

20 Leung, L. R., and Y. Qian, 2009. Atmospheric rivers induced heavy precipitation and flooding  
21 in the western U.S. simulated by the WRF regional climate model. *Geophysical Research*  
22 *Letters*, 36, L03820, doi:10.1029/2008GL036445.

23 Liguori, S., Rico-Ramirez, M.A. 2012. Quantitative assessment of short-term rainfall forecasts  
24 from radar nowcasts and MM5 forecasts. *Hydrological Processes*, vol 26., pp. 3842-3857

25 Liguori, S., Rico-Ramirez, M.A., Schellart, A., Saul, A. 2012, Using probabilistic radar rainfall  
26 nowcasts and NWP forecasts for flow prediction in urban catchments. *Atmospheric Research*,  
27 vol 103., pp. 80 – 95

28 Lo, J. C. F., Z. L. Yang, and R. A. Pielke Sr., 2008. Assessment of three dynamical climate  
29 downscaling methods using the Weather Research and Forecasting (WRF) model. *Journal of*  
30 *Geophysical Research*, 113, D09112, doi:10.1029/2007JD009216.

- 1 Milly P.C.D., Wetherland, R.T., Dunne, K.A., Delworth, T.L. 2002. Increasing risk of great  
2 floods in a changing climate. *Nature*, Vol.415, 514-517, doi :10.1038/415514a
- 3 Pappenberger, F., Beven, K. J., Hunter, N. M., Bates P. D., Gouweleeuw, B. T., Thielen, J., de  
4 Roo. A. P. J. 2005. Cascading model uncertainty from medium range weather forecasts (10  
5 days) through a rainfall-runoff model to flood inundation predictions within the European Flood  
6 Forecasting System (EFFS), *Hydrology and Earth System Sciences*, 9(4), pp. 381-393.  
7 doi:10.5194/hess-9-381-2005
- 8 Pappenberger, F., J. Bartholmes, J. Thielen, H. L. Cloke, R. Buizza, and A. de Roo (2008), New  
9 dimensions in early flood warning across the globe using grand-ensemble weather predictions,  
10 *Geophys. Res. Lett.*, 35, L10404, doi:10.1029/2008GL033837.
- 11 Pappenberger, F., Dutra, E., Wetterhall, F., Cloke, H. 2012. Deriving global flood hazard maps  
12 of fluvial floods through a physical model cascade. *Hydrology and Earth System Sciences*, 16  
13 4143–56.
- 14 Pedrozo-Acuña, A., Breña-Naranjo, J.A., Domínguez-Mora, R.—*accepted.*, 2014. The  
15 hydrological setting of the 2013 floods in Mexico, *Weather*, Vol.69, No.11, 295-302 Wiley  
16 and Sons. doi: 10.1002/wea.2355
- 17 Pedrozo-Acuña A., Mariño-Tapia I., Enriquez Ortiz C., Medellín Mayoral G., González-  
18 Villareal F.J. 2011. Evaluation of inundation areas resulting from the diversion of an extreme  
19 discharge towards the sea: case study in Tabasco, Mexico. *Hydrological Processes*, 26, (5),  
20 687–704.
- 21 Pedrozo-Acuña, A., Rodríguez-Rincón, J.P., Arganis-Juárez, M., Domínguez-Mora, R. and  
22 González Villareal, F.J. 2013. Estimation of probabilistic flood inundation maps for an extreme  
23 event: Pánuco River, México. *Journal of Flood Risk Management*, doi: 10.1111/jfr3.12067
- 24 Pedrozo-Acuña, A., Ruiz de Alegria-Arzaburu, A., Mariño-Tapia, I., Enriquez, C., González-  
25 Villareal, F.J. 2012. Factors controlling flooding at the Tonalá river mouth (Mexico). *Journal*  
26 *of Flood Risk Management*, Vol.5 (3) pp 226-244. doi: 10.1111/j.1753-318X.2012.01142.x
- 27 Pedrozo-Acuña, A. Mejía-Estrada P.I., Rodríguez-Rincón, J.P., Domínguez-Mora, R.,  
28 González-Villareal, F.J., Flood Risk From Extreme Events in Mexico, 11th International  
29 Conference on Hydroinformatics, ~~2014~~2014b.

1 Prinos P., Kortenhaus A., Swerpel B. & Jiménez J.A. 2008. Review of flood hazard mapping.  
2 Floodsite Report No. T03-07-01, 54.

3 Qian, J.-H., A. Seth, and S. Zebiak 2003. Reinitialized versus continuous simulations for  
4 regional climate downscaling, *Mon. Weather Rev.*, 131, 2857–2874.

5 Rodríguez-Rincón, J.P., Pedrozo-Acuña, A., Domínguez Mora, R., Reeve, D.E., Cluckie, I.  
6 2012. Probabilistic estimation of flood maps: An ensemble approach. *FloodRisk2012*, The 2nd  
7 European Conference on FLOODrisk Management.

8 Skamarock, W.C., Klemp, J.B., Dudhia, J., Gill, D.O., Barker, D.M., Duda, M.G., Huang, X.-  
9 Y., Wang, W., Powers, J.G. 2008. *A description of the Advanced Research WRF version3*.  
10 NCAR Technical Note NCAR/TN475+STR.

11 Slingo, J., Belcher, S., Scafie, A., McCarthy, M., Saulter, A., McBeath, K., Jenkins, A.,  
12 Huntingford, C., Marsh, T., Hannaford, J., Parry, S. 2014. The recent storms and floods in the  
13 UK. Report Met Office and CEH.

14 Teutschbein C, Seibert J. 2010. Regional climate models for hydrological impact studies at the  
15 catchment scale: a review of recent modelling strategies. *Geography Compass* 4: 834–860.

16 [USDA-SCS. 1985. National Engineering Handbook, Section 4 - Hydrology. Washington, D.C.:](#)  
17 [USDA-SCS.](#)

18 Ushiyama, T., Sayama, T., Tatebe, Y., Fujioka, S., Fukami, K., 2014. Numerical simulation of  
19 2010 Pakistan Flood in the Kabul river basin by using lagged ensemble rainfall forecasting,  
20 *Journal of Hydrometeorology*, Vol. 15, 193-211 pp., doi: 10.1175/JHM-D-13-011.1.

21 [Ven den Honert, R. C. & McAneney, J. 2011. The 2011 Brisbane floods: Causes, impacts and](#)  
22 [implications. \*Water\* 3, 1149–1173.](#)

23 Wang, W., Bruyere, C., Duda, M., Dudhia, J., Gill, D., Lin, H. C., & Mandel, J.. *ARW version*  
24 *3 modeling system user's guide*. Mesoscale & Microscale Meteorology Division. National  
25 Center for Atmospheric Research (July 2010), [http://www.mmm.ucar.edu/wrf/users/docs/user\\_guide\\_V3/ARWUsersGuideV3.pdf](http://www.mmm.ucar.edu/wrf/users/docs/user_guide_V3/ARWUsersGuideV3.pdf).

26

27 Ward, P. J., De Moel, H., and Aerts, J. C. J. H. 2011 How are flood risk estimates affected by  
28 the choice of return-periods? *Nat. Hazards Earth Syst. Sci.* 11 3181–95.

29 [Webster, P. J., Toma, V. E. & Kim, H. M. 2011. Were the 2010 Pakistan floods predictable?](#)  
30 [\*Geophys. Res. Lett.\* 38, L04806.](#)

- 1 Werner, M.G.F., Hunter, N. and Bates, P.D. 2005. Identifiability of distributed floodplain  
2 roughness values in flood extent estimation, J. Hydrol., 314, 139–157.
- 3 World Meteorological Organization, 2011. Provisional Statement on the Status of the Global  
4 Climate; available [http://www.wmo.int/pages/mediacentre/press\\_releases/gcs\\_2011\\_en.html](http://www.wmo.int/pages/mediacentre/press_releases/gcs_2011_en.html)
- 5 Wright, N. G., Asce, M., Villanueva, I., et al. (2008). Case study of the use of remotely sensed  
6 data for modeling flood inundation on the River Severn, UK. Journal of Hydraulic Engineering,  
7 134(5), 533–540.
- 8 Ye, J., He, Y., Pappenberger, F., Cloke, H. L., Manful, D. Y. and Li, Z. (2014), Evaluation of  
9 ECMWF medium-range ensemble forecasts of precipitation for river basins. Q.J.R. Meteorol.  
10 Soc., 140: 1615–1628. doi: 10.1002/qj.2243
- 11

1

2

Table 1. Ensemble members defined for the multi-physics WRF ensemble

<b>Ensemble member</b>	<b>Micro-Physics</b>	<b>surface layer physics</b>	<b>Cumulus physics</b>	<b>Feedback/sst_update</b>
1	WSM5	5-Layer TDM	Kain-Fritsch Eta	off/on
2	WSM5	5-Layer TDM	Kain-Fritsch Eta	on/off
3	WSM5	5-Layer TDM	Kain-Fritsch Eta	on/on
4	WSM5	Noah	Kain-Fritsch Eta	off/off
5	WSM5	Noah	Kain-Fritsch Eta	off/on
6	WSM5	Noah	Kain-Fritsch Eta	on/on
7	Thompson	5-Layer TDM	Kain-Fritsch Eta	off/off
8	Thompson	5-Layer TDM	Kain-Fritsch Eta	off/on
9	Thompson	5-Layer TDM	Kain-Fritsch Eta	on/off
10	Thompson	5-Layer TDM	Kain-Fritsch Eta	on/on
11	Thompson	Noah	Kain-Fritsch Eta	off/off
12	Thompson	Noah	Kain-Fritsch Eta	off/on

3

4

5

6

7

8

9

10

11

12

13

14

15

1 Table 2. Error Metrics in the estimation of precipitation by members of the multi-physics ensemble (blue rows  
 2 indicate the stations located within the Tonalá catchment)

Root-Mean Square Error (RMSE) and Normalised RMSE per Station considering Ensemble average													
Station No.	Multi-physics ensemble member												<Nor_RMSE> %
	M1	M2	M3	M4	M5	M6	M7	M8	M9	M10	M11	M12	
30167	210.26	96.56	144.62	104.42	106.84	76.31	160.48	129.88	101.03	210.95	164.85	86.80	13.96
27003	544.34	578.19	564.46	474.81	427.30	516.95	458.25	484.05	568.20	572.30	385.17	479.47	35.13
27007	234.90	246.00	198.01	135.27	129.43	207.93	126.51	197.32	246.90	328.28	132.09	191.81	19.44
27015	96.68	129.89	151.02	194.33	235.76	179.69	152.06	152.60	118.97	116.87	260.49	188.20	24.01
27074	173.37	211.87	191.22	197.46	78.94	148.88	174.92	247.65	187.98	207.39	123.09	157.21	17.19
27073	227.47	201.91	228.62	256.39	281.38	245.68	186.21	219.36	159.34	147.79	247.69	223.88	46.46
27075	87.04	119.26	104.10	100.82	151.17	64.92	76.45	147.30	85.75	105.68	52.14	68.67	10.72
27076	140.53	160.28	141.95	124.03	108.33	130.53	191.75	162.59	226.04	236.09	129.78	150.84	17.14
27077	89.10	113.42	83.60	225.48	252.24	207.73	254.20	282.40	110.77	83.93	203.01	192.86	30.57
27039	333.50	204.36	197.48	295.84	302.19	261.39	264.08	321.66	172.86	152.14	257.59	430.63	73.28
27054	123.18	30.77	45.28	113.16	119.18	77.41	106.84	112.68	118.83	127.43	110.06	106.67	34.75
27060	70.69	56.23	59.51	33.42	40.13	30.04	78.07	93.80	88.46	80.36	56.73	66.31	19.88
27024	160.33	137.81	140.76	120.58	127.54	73.57	148.27	136.47	145.12	167.79	153.26	151.87	85.04
27084	68.72	71.32	54.58	53.56	106.93	65.65	61.06	72.31	61.46	62.96	50.14	50.92	19.02
7365	172.91	117.44	103.02	252.03	139.79	163.49	301.52	216.38	179.67	129.71	271.88	210.11	24.52
27011	143.70	162.77	143.61	107.82	77.55	86.15	128.03	143.69	106.59	116.49	86.81	81.27	106.83
27036	81.46	60.69	27.36	61.69	19.14	35.64	23.58	45.89	22.13	40.23	39.22	55.55	12.04
27008	158.85	72.82	74.96	131.34	134.94	100.16	102.82	149.97	66.67	79.36	97.87	254.33	19.68
Average {Rel_RMSE} catch.												23.14	
Average {Rel_RMSE} all												33.87	

BIAS per Station and Ensemble Average													
Station No.	Multi-physics ensemble member												<BIAS>
	M1	M2	M3	M4	M5	M6	M7	M8	M9	M10	M11	M12	
30167	0.71	0.90	0.81	1.07	1.12	0.99	0.80	0.85	0.91	0.71	1.23	1.06	0.93
27003	0.51	0.48	0.50	0.58	0.62	0.54	0.59	0.57	0.49	0.49	0.66	0.58	0.55
27007	0.72	0.71	0.79	0.91	0.91	0.78	1.13	1.26	0.73	0.61	0.90	0.80	0.85
27015	1.21	1.32	1.40	1.50	1.61	1.46	1.37	1.37	1.24	1.21	1.68	1.48	1.40
27074	0.82	0.76	0.79	0.78	1.08	0.86	0.81	0.71	0.80	0.77	0.88	0.83	0.82
27073	1.74	1.65	1.74	1.83	1.91	1.80	1.58	1.70	1.47	1.44	1.80	1.72	1.70
27075	0.92	0.85	0.88	0.88	1.20	0.96	0.90	0.80	0.89	0.86	0.98	0.93	0.92
27076	0.86	0.82	0.86	0.91	0.95	0.89	0.79	0.84	0.73	0.71	0.89	0.85	0.84
27077	1.12	1.17	1.10	1.48	1.54	1.44	1.54	1.60	1.20	1.14	1.42	1.40	1.35
27039	2.41	1.87	1.84	2.26	2.29	2.11	2.13	2.36	1.73	1.64	2.09	2.84	2.13
27054	1.89	1.08	1.24	1.82	1.87	1.54	1.76	1.81	1.84	1.91	1.79	1.77	1.69
27060	1.42	1.33	0.72	1.08	1.20	1.05	1.47	1.57	1.54	1.49	1.32	1.39	1.30
27024	3.34	2.96	3.03	2.76	2.88	2.07	3.16	2.98	3.11	3.45	3.17	3.17	3.01
27084	1.32	1.35	1.17	1.23	1.61	0.78	1.27	1.36	1.27	1.29	1.07	1.01	1.23
7365	1.43	1.20	1.09	1.63	1.32	0.72	1.78	1.55	1.43	1.26	1.68	1.51	1.38
27011	3.57	3.91	3.55	2.93	2.33	2.49	3.33	3.58	2.91	3.09	2.56	2.45	3.06
27036	1.36	1.25	1.09	1.28	0.97	1.15	0.95	1.20	1.06	1.16	1.15	1.24	1.15
27008	1.37	1.07	1.05	1.29	1.31	1.20	1.21	1.35	0.99	0.93	1.19	1.62	1.22
Average {Rel_RMSE} catch.												0.94	
Average {Rel_RMSE} all												1.42	

3  
 4  
 5  
 6



1 Continuation of Table 2. Error Metrics in the estimation of precipitation by members of the multi-physics  
 2 ensemble (blue rows indicate the stations located within the Tonalá catchment)  
 3

Nash-Sutcliff Coefficient per Station and Ensemble average													
Station No.	Multi-physics ensemble member												<NSC>
	M1	M2	M3	M4	M5	M6	M7	M8	M9	M10	M11	M12	
<b>30167</b>	0.72	0.94	0.87	0.93	0.93	0.96	0.84	0.89	0.94	0.72	0.83	0.95	<b>0.88</b>
<b>27003</b>	0.16	0.05	0.09	0.36	0.48	0.24	0.40	0.33	0.08	0.07	0.58	0.34	<b>0.26</b>
<b>27007</b>	0.70	0.67	0.78	0.90	0.91	0.76	0.91	0.79	0.66	0.41	0.90	0.80	<b>0.77</b>
<b>27015</b>	0.88	0.78	0.70	0.50	0.27	0.57	0.70	0.69	0.81	0.82	0.11	0.53	<b>0.61</b>
27074	0.84	0.76	0.80	0.79	0.97	0.88	0.84	0.67	0.81	0.77	0.92	0.87	0.83
27073	-0.27	0.00	-0.28	-0.61	-0.94	-0.48	0.15	-0.18	0.38	0.46	-0.50	-0.23	-0.21
<b>27075</b>	<b>0.94</b>	<b>0.89</b>	<b>0.91</b>	<b>0.92</b>	<b>0.82</b>	<b>0.97</b>	<b>0.95</b>	<b>0.83</b>	<b>0.94</b>	<b>0.91</b>	<b>0.98</b>	<b>0.96</b>	<b>0.92</b>
27076	0.87	0.83	0.86	0.90	0.92	0.88	0.75	0.82	0.65	0.62	0.89	0.85	0.82
27077	0.82	0.70	0.84	-0.17	-0.46	0.01	-0.48	-0.83	0.72	0.84	0.05	0.15	0.18
27039	-4.41	-1.03	-0.90	-3.26	-3.44	-2.32	-2.39	-4.03	-0.45	-0.13	-2.23	-8.02	-2.72
27054	-0.46	0.91	0.80	-0.23	-0.36	0.42	-0.10	-0.22	-0.36	-0.56	-0.16	-0.09	-0.03
27060	0.60	0.75	0.72	0.91	0.87	0.93	0.51	0.29	0.37	0.48	0.74	0.65	0.65
27024	-7.99	-5.64	-5.93	-4.08	-4.69	-0.89	-6.68	-5.51	-6.36	-8.84	-7.21	-7.06	-5.91
27084	0.67	0.64	0.79	0.80	0.20	0.70	0.74	0.63	0.73	0.72	0.82	0.82	0.69
7365	0.50	0.77	0.82	-0.07	0.67	0.55	-0.54	0.21	0.45	0.72	-0.25	0.25	0.34
27011	-16.74	-21.76	-16.72	-8.99	-4.17	-5.38	-13.08	-16.74	-8.76	-10.66	-5.47	-4.67	-11.09
27036	0.61	0.78	0.96	0.78	0.98	0.93	0.97	0.88	0.97	0.91	0.91	0.82	0.87
27008	0.60	0.92	0.91	0.72	0.71	0.84	0.83	0.64	0.93	0.90	0.85	-0.03	0.73
Average {Rel_RMSE} catch.												<b>0.63</b>	
Average {Rel_RMSE} all												-0.63	

Correlation Coefficient per Station and Ensemble average													
Station No.	Multi-physics ensemble member												<Cor>
	M1	M2	M3	M4	M5	M6	M7	M8	M9	M10	M11	M12	
<b>30167</b>	<b>0.99</b>	<b>0.99</b>	<b>0.99</b>	<b>0.97</b>	<b>0.98</b>	<b>0.99</b>	<b>0.99</b>	<b>0.99</b>	<b>0.99</b>	<b>0.99</b>	<b>0.97</b>	<b>0.98</b>	<b>0.99</b>
<b>27003</b>	<b>0.95</b>	<b>0.96</b>	<b>0.97</b>	<b>0.97</b>	<b>0.98</b>	<b>0.98</b>	<b>0.99</b>	<b>0.99</b>	<b>0.99</b>	<b>0.99</b>	<b>0.99</b>	<b>0.99</b>	<b>0.98</b>
<b>27007</b>	<b>0.98</b>	<b>0.97</b>	<b>0.97</b>	<b>0.97</b>	<b>0.97</b>	<b>0.97</b>	<b>0.97</b>	<b>0.97</b>	<b>0.97</b>	<b>0.95</b>	<b>0.98</b>	<b>0.97</b>	<b>0.97</b>
<b>27015</b>	<b>0.97</b>	<b>0.96</b>	<b>0.97</b>	<b>0.94</b>	<b>0.93</b>	<b>0.95</b>	<b>0.95</b>	<b>0.95</b>	<b>0.94</b>	<b>0.94</b>	<b>0.93</b>	<b>0.94</b>	<b>0.95</b>
27074	0.98	0.98	0.98	0.98	0.99	0.98	0.99	0.98	0.98	0.98	0.99	0.99	0.98
27073	0.95	0.96	0.95	0.94	0.94	0.94	0.92	0.92	0.91	0.92	0.94	0.94	0.94
<b>27075</b>	0.98	0.98	0.98	0.98	0.99	0.99	0.99	0.99	0.99	0.99	0.99	0.99	<b>0.99</b>
27076	0.98	0.98	0.97	0.97	0.97	0.97	0.97	0.97	0.96	0.96	0.97	0.97	0.97
27077	0.96	0.95	0.96	0.96	0.95	0.96	0.95	0.95	0.97	0.97	0.95	0.96	0.96
27039	0.95	0.95	0.94	0.93	0.94	0.94	0.94	0.94	0.95	0.95	0.94	0.93	0.94
27054	0.91	0.96	0.94	0.93	0.93	0.94	0.91	0.92	0.91	0.90	0.93	0.93	0.93
27060	0.96	0.97	0.97	0.96	0.97	0.97	0.95	0.95	0.96	0.96	0.97	0.96	0.96
27024	0.91	0.93	0.92	0.90	0.91	0.95	0.89	0.90	0.89	0.89	0.94	0.94	0.91
27084	0.91	0.91	0.92	0.94	0.92	0.95	0.92	0.91	0.92	0.92	0.93	0.93	0.92
7365	0.93	0.93	0.94	0.92	0.94	0.97	0.91	0.92	0.91	0.92	0.91	0.92	0.93
27011	0.94	0.94	0.95	0.93	0.95	0.96	0.89	0.93	0.91	0.92	0.91	0.91	0.93
27036	0.99	0.99	0.99	0.99	0.99	0.99	0.99	0.99	0.99	0.99	0.99	0.99	0.99
27008	0.97	0.96	0.96	0.96	0.96	0.96	0.96	0.96	0.97	0.96	0.96	0.96	0.96
Average {Rel_RMSE} catch.												<b>0.97</b>	
Average {Rel_RMSE} all												0.95	

4

1  
2  
3  
4  
5  
6  
7  
8  
9  
10  
11

Table 3. Flood events in the Tonalá River used in the calibration process of free parameters in the hydrological model, along with computed error metrics.

Event	Max Q (m <sup>3</sup> /s) Obs.	$\lambda$	Fs	Fo	Max Q (m <sup>3</sup> /s) Calc.	NSC	Cor	Bias
2001	577.98	0.2	0.1	0.9	584.79	0.529	0.764	1.112
2005	589.25	0.4	0.6	0.9	609.87	0.812	0.907	1.043
2007	538.50	0.2	1.8	0.9	543.87	0.483	0.780	0.902
2008	597.35	0.4	1.8	0.9	823.04	0.155	0.861	0.983
2009	1262.57	0.8	1.8	0.9	1424.56	0.910	0.962	0.942
2011	545.40	0.9	1.6	0.9	597.08	0.413	0.721	1.051

Table 4. Error metrics in the estimation of river discharge by the rainfall-runoff model using the 6 parameter sets and 12 members of the multi-physics ensemble.

-	<b>Error metrics per ensemble member and ensemble average for the hydrological model</b>										
	<b>M1</b>	<b>M2</b>	<b>M3</b>	<b>M4</b>	<b>M5</b>	<b>M6</b>	<b>M7</b>	<b>M8</b>	<b>M9</b>	<b>M10</b>	<b>M11</b>
<b>RMSE (m<sup>3</sup>/s)</b>	163.05	122.49	110.53	230.13	201.49	153.81	147.25	131.42	123.96	127.51	232.76
<b>NSC</b>	0.84	0.91	0.93	0.69	0.76	0.86	0.87	0.90	0.91	0.90	0.68
<b>Cor</b>	0.97	0.98	0.98	0.97	0.95	0.96	0.95	0.96	0.96	0.96	0.94
<b>BIAS</b>	0.83	0.89	0.92	1.29	1.20	0.86	1.08	0.90	0.94	0.94	1.24
<b>NRMSE (%)</b>	39.75	29.86	26.95	56.11	49.12	37.50	35.90	32.04	30.22	31.09	56.75

(those selected are shown in bold with NSC>0.6 and Cor>0.7).

Member No.	WRF Member	Hydrological Parameters	NSC	Cor	Bias
1	<b>M1</b>	<b>2001</b>	<b>0.733</b>	<b>0.884</b>	<b>0.852</b>
2	M2	2001	0.074	0.973	1.529
3	M3	2001	-0.035	0.974	1.564
4	M4	2001	-0.511	0.975	1.686
5	M5	2001	-0.638	0.441	1.485
6	M6	2001	-0.223	0.961	1.593
7	M7	2001	-0.192	0.961	1.579
8	M8	2001	-0.043	0.959	1.537
9	M9	2001	0.064	0.958	1.504
10	M10	2001	0.245	0.971	0.525
11	M11	2001	-1.503	0.944	1.832
12	M12	2001	-0.752	0.954	1.710
13	<b>M1</b>	<b>2005</b>	<b>0.639</b>	<b>0.901</b>	<b>0.742</b>
14	M2	2005	0.404	0.977	1.414
15	M3	2005	0.318	0.978	1.449
16	M4	2005	-0.077	0.977	1.569
17	M5	2005	-0.545	0.366	1.368
18	M6	2005	0.181	0.968	1.478
19	M7	2005	0.200	0.968	1.465
20	M8	2005	0.321	0.966	1.422
21	M9	2005	0.408	0.966	1.389
22	M10	2005	-0.081	0.960	0.426
23	M11	2005	-0.909	0.951	1.717
24	M12	2005	-0.264	0.961	1.595
25	M1	2007	0.376	0.914	0.601
26	<b>M2</b>	<b>2007</b>	<b>0.761</b>	<b>0.978</b>	<b>1.244</b>
27	<b>M3</b>	<b>2007</b>	<b>0.711</b>	<b>0.979</b>	<b>1.278</b>
28	M4	2007	0.444	0.976	1.395
29	M5	2007	-0.440	0.261	1.191
30	<b>M6</b>	<b>2007</b>	<b>0.633</b>	<b>0.974</b>	<b>1.306</b>
31	<b>M7</b>	<b>2007</b>	<b>0.647</b>	<b>0.974</b>	<b>1.293</b>
32	<b>M8</b>	<b>2007</b>	<b>0.722</b>	<b>0.973</b>	<b>1.251</b>
33	<b>M9</b>	<b>2007</b>	<b>0.771</b>	<b>0.972</b>	<b>1.219</b>
34	M10	2007	-0.508	0.952	0.322
35	M11	2007	-0.129	0.959	1.539
36	M12	2007	0.340	0.969	1.420
37	M1	2008	0.240	0.922	0.547
38	<b>M2</b>	<b>2008</b>	<b>0.837</b>	<b>0.978</b>	<b>1.186</b>
39	<b>M3</b>	<b>2008</b>	<b>0.797</b>	<b>0.978</b>	<b>1.220</b>
40	M4	2008	0.570	0.974	1.337
41	M5	2008	-0.479	0.209	1.132
42	<b>M6</b>	<b>2008</b>	<b>0.741</b>	<b>0.976</b>	<b>1.248</b>
43	<b>M7</b>	<b>2008</b>	<b>0.753</b>	<b>0.976</b>	<b>1.235</b>
44	<b>M8</b>	<b>2008</b>	<b>0.813</b>	<b>0.975</b>	<b>1.194</b>
45	<b>M9</b>	<b>2008</b>	<b>0.851</b>	<b>0.975</b>	<b>1.161</b>
46	M10	2008	-0.720	0.945	0.276
47	M11	2008	0.079	0.962	1.481
48	<b>M12</b>	<b>2008</b>	<b>0.495</b>	<b>0.972</b>	<b>1.361</b>
49	M1	2009	-0.036	0.838	0.494
50	<b>M2</b>	<b>2009</b>	<b>0.819</b>	<b>0.978</b>	<b>0.882</b>
51	<b>M3</b>	<b>2009</b>	<b>0.899</b>	<b>0.977</b>	<b>0.907</b>
52	<b>M4</b>	<b>2009</b>	<b>0.649</b>	<b>0.963</b>	<b>1.286</b>
53	M5	2009	0.060	0.811	0.580
54	<b>M6</b>	<b>2009</b>	<b>0.839</b>	<b>0.959</b>	<b>0.849</b>
55	<b>M7</b>	<b>2009</b>	<b>0.883</b>	<b>0.959</b>	<b>0.890</b>
56	<b>M8</b>	<b>2009</b>	<b>0.896</b>	<b>0.954</b>	<b>0.929</b>
57	<b>M9</b>	<b>2009</b>	<b>0.890</b>	<b>0.950</b>	<b>0.928</b>
58	M10	2009	-1.233	0.972	0.209
59	<b>M11</b>	<b>2009</b>	<b>0.638</b>	<b>0.938</b>	<b>1.236</b>
60	<b>M12</b>	<b>2009</b>	<b>0.885</b>	<b>0.946</b>	<b>1.042</b>
61	M1	2011	-0.247	0.949	0.396
62	<b>M2</b>	<b>2011</b>	<b>0.938</b>	<b>0.970</b>	<b>1.019</b>
63	<b>M3</b>	<b>2011</b>	<b>0.930</b>	<b>0.971</b>	<b>1.052</b>
64	<b>M4</b>	<b>2011</b>	<b>0.819</b>	<b>0.964</b>	<b>1.168</b>
65	M5	2011	-0.662	0.055	0.955
66	<b>M6</b>	<b>2011</b>	<b>0.890</b>	<b>0.978</b>	<b>1.133</b>
67	<b>M7</b>	<b>2011</b>	<b>0.899</b>	<b>0.979</b>	<b>1.120</b>
68	<b>M8</b>	<b>2011</b>	<b>0.931</b>	<b>0.979</b>	<b>1.079</b>
69	<b>M9</b>	<b>2011</b>	<b>0.945</b>	<b>0.978</b>	<b>1.047</b>
70	M10	2011	-1.136	0.931	0.195
71	M11	2011	0.433	0.967	1.364
72	<b>M12</b>	<b>2011</b>	<b>0.738</b>	<b>0.976</b>	<b>1.246</b>
<Ensemble average of selected members>			0.793	0.965	1.113

1  
2  
3

Table 45. Error metrics in the estimation of river discharge by the hydrodynamic model using the 1231 members of the multi-physics ensemble.

- Comparison of flooded areas between numerical results from running ensemble members vs. Observed													
Error metrics	Ensemble Member												<Ensemble average>
	M1	M2	M3	M4	M5	M6	M7	M8	M9	M10	M11	M12	
<b>BIAS</b>	0.872	0.893	0.904	0.917	0.910	0.872	0.940	1.006	1.022	1.073	1.040	1.119	0.964
<b>FAR: False Alarm Ratio</b>	0.132	0.143	0.148	0.154	0.149	0.132	0.562	0.817	0.824	0.847	0.865	0.877	0.453
<b>POD: Probability of Detection</b>	0.757	0.765	0.770	0.776	0.750	0.757	0.782	0.817	0.824	0.847	0.856	0.877	0.799
<b>POFD: Probability of False Detection</b>	0.107	0.119	0.125	0.132	0.112	0.107	0.145	0.176	0.185	0.210	0.205	0.225	0.154
<b>CSI: Critical Success Index</b>	0.868	0.857	0.852	0.846	0.851	0.868	0.834	0.812	0.806	0.790	0.791	0.784	0.831
<b>True Skill Statistics</b>	0.650	0.646	0.645	0.644	0.653	0.650	0.645	0.641	0.639	0.637	0.641	0.652	0.645

4

1  
2

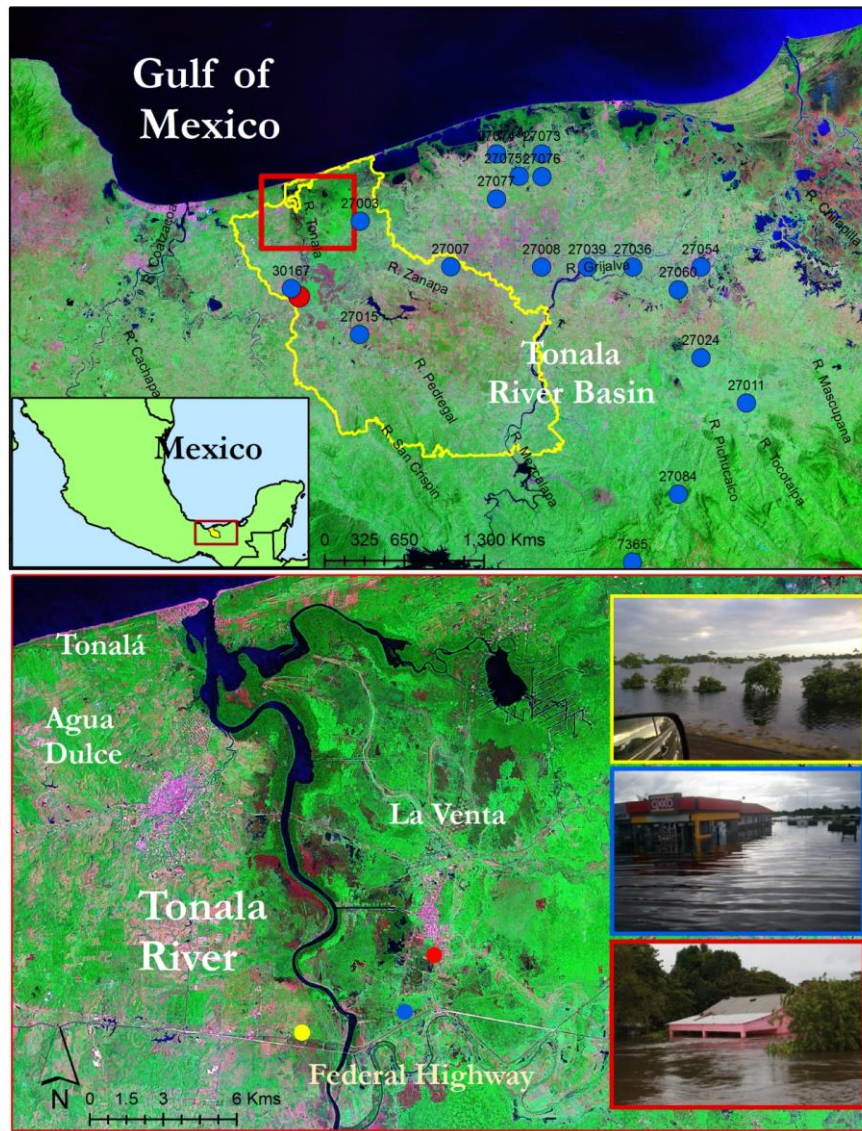


Comparison of flooded areas between numerical results from running ensemble members vs. Observed																																
Error metrics	Ensemble Member																												<Ensemble average>			
	M1	M13	M26	M27	M30	M31	M32	M33	M38	M39	M42	M43	M44	M45	M50	M51	M52	M54	M55	M56	M57	M59	M60	M62	M63	M64	M66	M67		M68	M69	M72
<b>BIAS</b>	0.903	0.838	1.084	1.099	1.119	1.120	1.094	1.078	1.056	1.021	1.092	1.089	1.096	1.051	0.902	0.915	0.891	0.820	1.020	0.982	0.872	1.056	1.004	0.982	0.995	1.047	1.040	1.028	1.016	1.005	1.092	1.013
<b>FAR: False Alarm Ratio</b>	0.148	0.120	0.215	0.217	0.283	0.210	0.216	0.212	0.209	0.217	0.216	0.215	0.152	0.207	0.148	0.154	0.139	0.137	0.193	0.155	0.133	0.206	0.187	0.178	0.182	0.204	0.201	0.225	0.192	0.187	0.216	0.189
<b>POD: Probability of Detection</b>	0.770	0.737	0.851	0.861	0.849	0.849	0.858	0.849	0.836	0.751	0.857	0.854	0.848	0.833	0.769	0.775	0.751	0.810	0.823	0.845	0.756	0.847	0.816	0.807	0.814	0.833	0.831	0.821	0.821	0.818	0.857	0.819
<b>POFD:Probability of False Detection</b>	0.124	0.094	0.217	0.222	0.187	0.187	0.220	0.214	0.205	0.186	0.220	0.219	0.186	0.203	0.124	0.131	0.185	0.185	0.184	0.066	0.108	0.266	0.175	0.163	0.168	0.199	0.195	0.186	0.182	0.175	0.220	0.180
<b>CSI : Critical Success Index</b>	0.679	0.670	0.690	0.695	0.711	0.711	0.694	0.691	0.685	0.709	0.693	0.692	0.710	0.685	0.679	0.679	0.706	0.654	0.687	0.708	0.677	0.620	0.687	0.687	0.690	0.686	0.687	0.619	0.688	0.688	0.693	0.686
<b>True Skill Statistics</b>	0.645	0.643	0.634	0.639	0.621	0.662	0.638	0.636	0.631	0.660	0.637	0.636	0.661	0.631	0.645	0.643	0.615	0.601	0.639	0.659	0.648	0.660	0.641	0.644	0.640	0.634	0.636	0.610	0.640	0.642	0.637	0.639

1

2

1  
2



3

4 **Figure 1.** Top panel: Location of the Tonalá River basin in Mexico, blue line represents the  
5 boundary limits of the catchment; blue dots illustrate the location of weather stations; red dot:  
6 streamflow gauge. Bottom panel: zoom of the study area and photographs of observed  
7 impacts; yellow, blue and red dots represent the location at which photos were taken.  
8



1

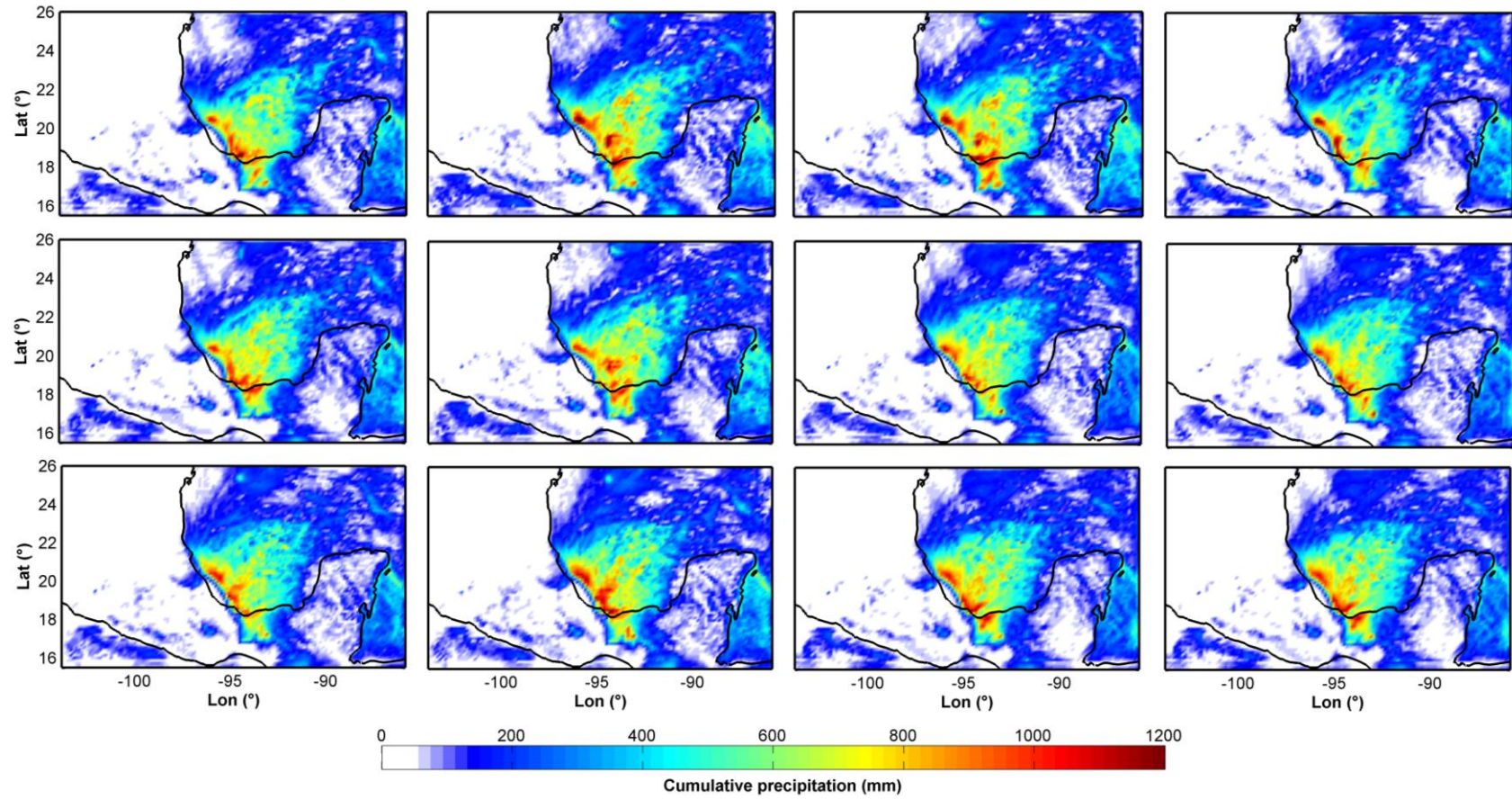
2



3

4 **Figure 2.** Numerical setup of the WRF with a nested domain covering Mexico. Domain 1:  
5 25km resolution; Domain 2: 4km resolution; the orange region illustrates the Tonalá  
6 catchment.

1



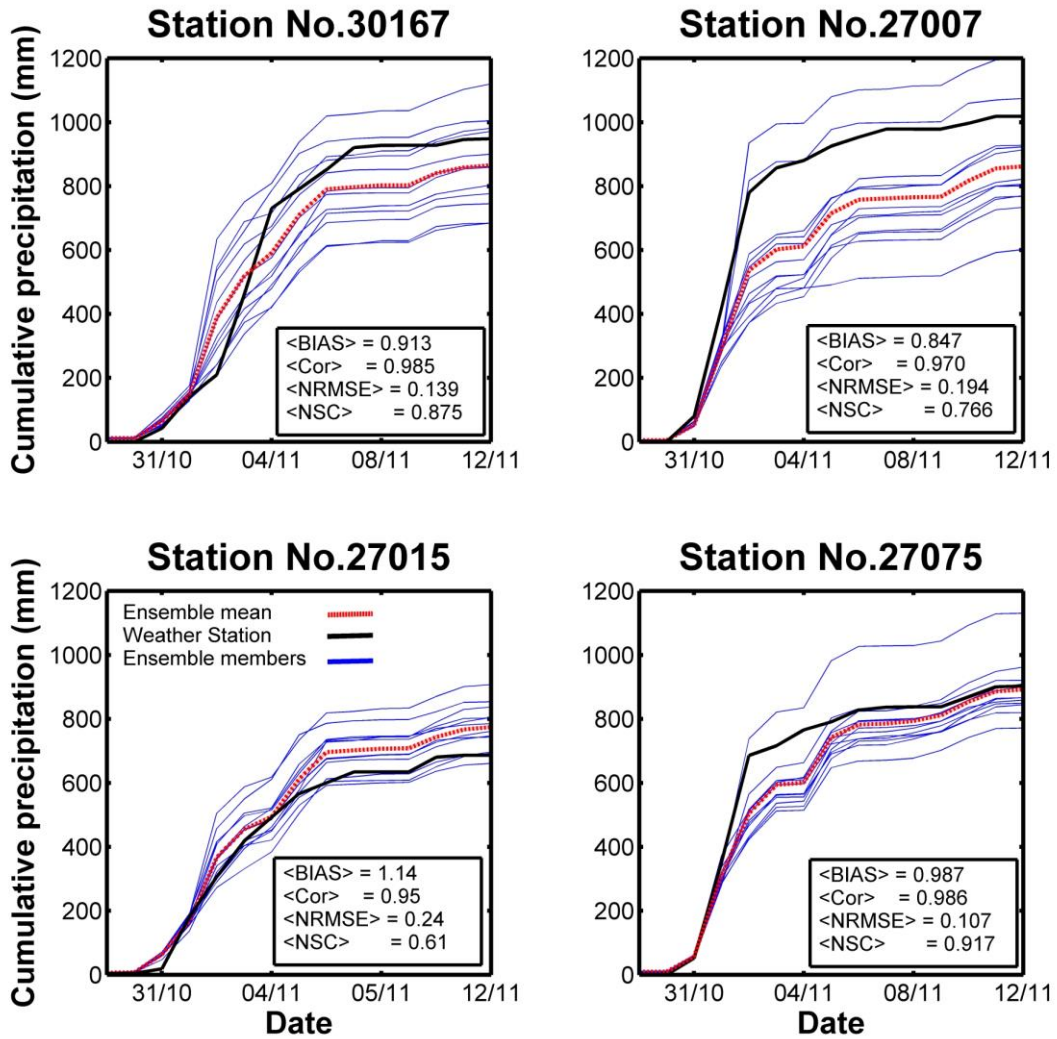
2

3

4

**Figure 3.** Cumulative precipitation fields estimated by the WRF model using the 12 members of the multi-physics ensemble (27<sup>th</sup> October 2009 – 12<sup>th</sup> November 2009).

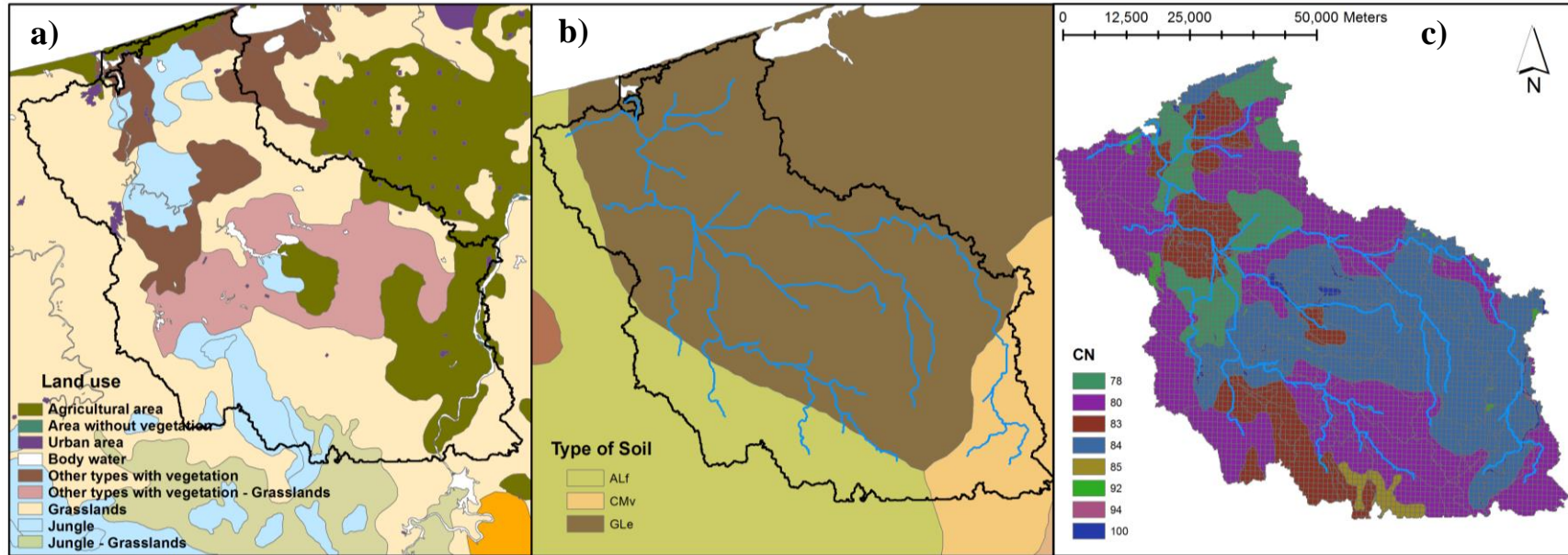
1  
2



3  
4  
5  
6

**Figure 4.** Comparison of cumulative precipitation estimated by the 12 members of the WRF model (blue lines) and its mean (red line) vs. measurements (black solid line) at four weather stations from 27<sup>th</sup> October 2009 to 12<sup>th</sup> November 2009.

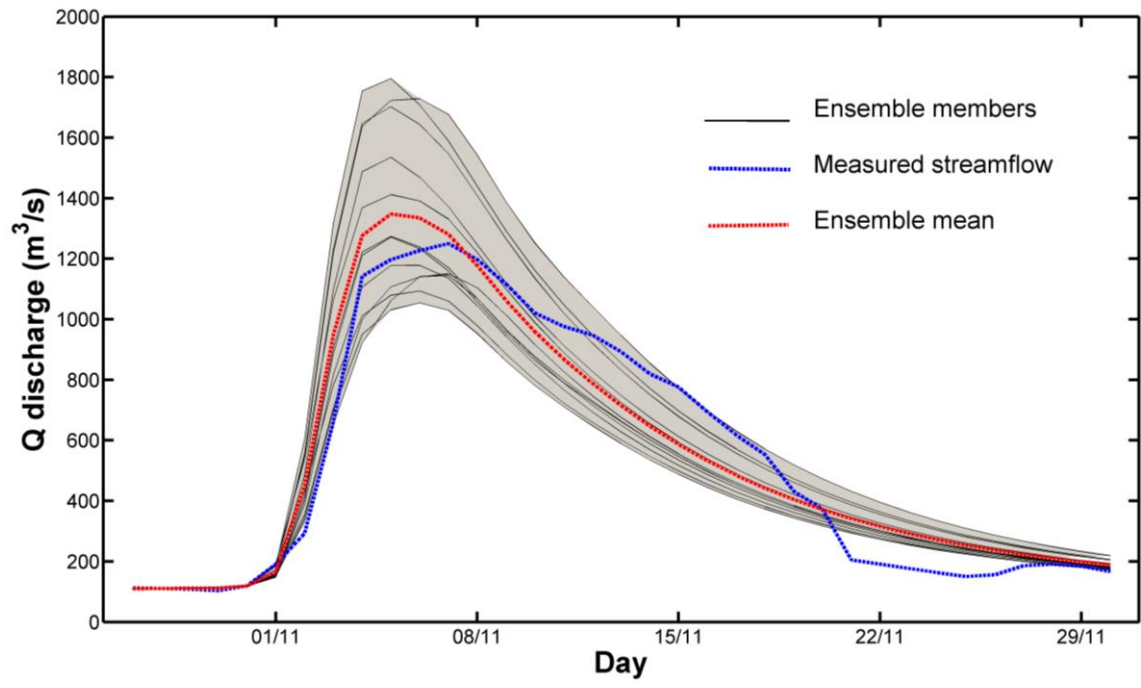
1  
2  
3



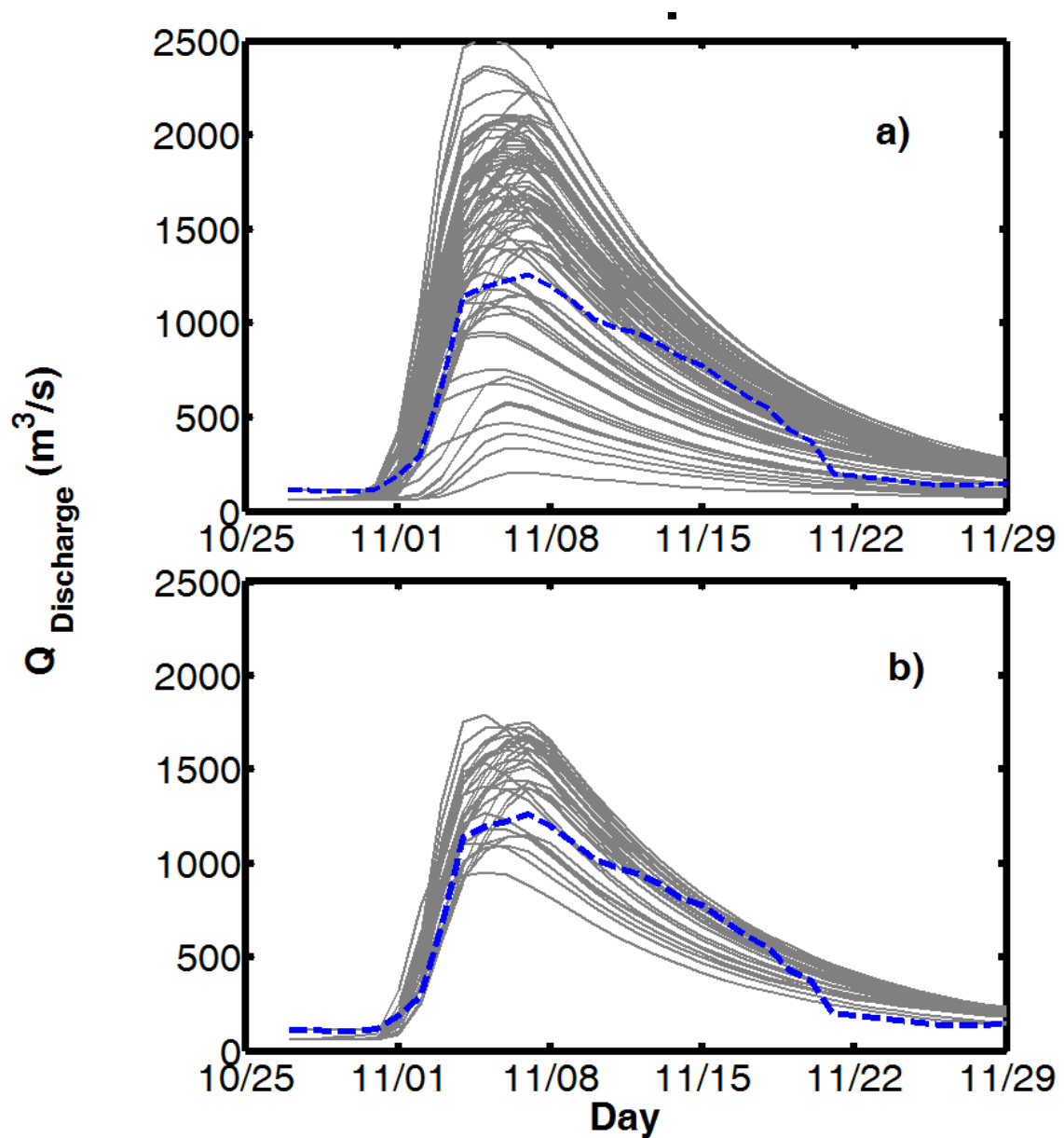
4  
5

**Figure 5.** Input data parameters in the hydrological model; a) Land use; b) Pedology; c) River network, curve number and grid.

1  
2  
3  
4



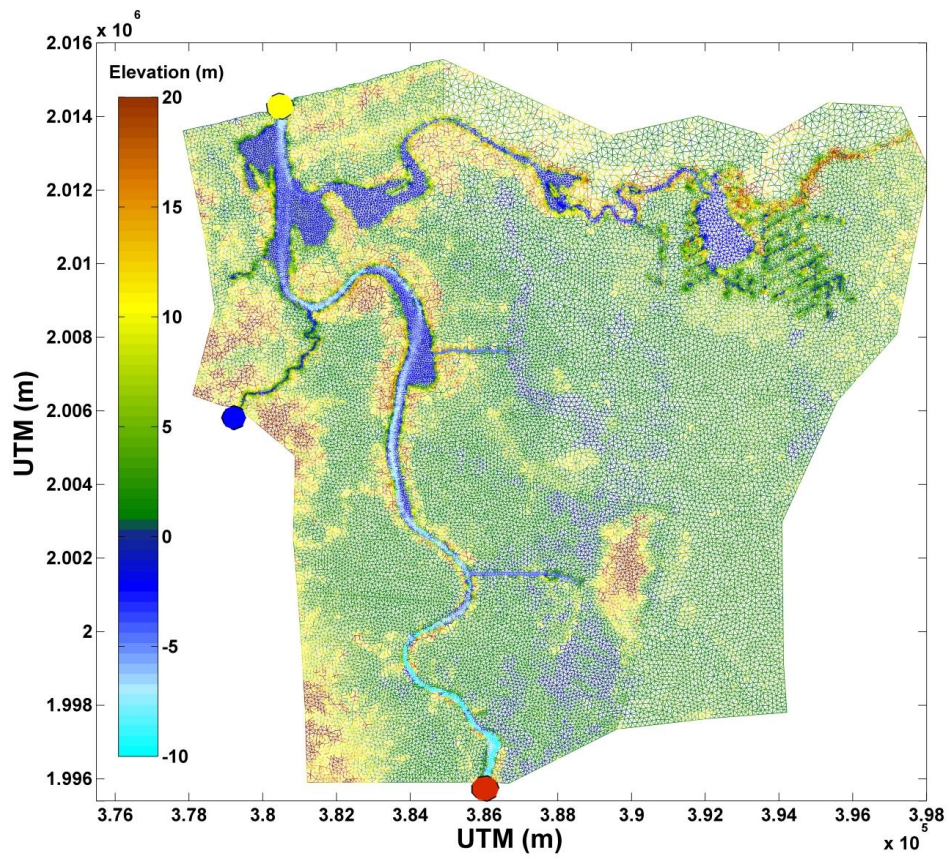
5



1  
2  
3  
4  
5  
6  
7

**Figure 6.** Calculated a) 72 hydrographs computed using the rainfall-runoff model with 6 sets of parameters and 12 WRF ensemble precipitation fields as input data; b) 31 selected hydrographs to serve as input in the hydrodynamic model; grey shaded area illustrates the uncertainty bounds (maximum and minimum); lines illustrate the red ensemble members and the blue dashed line shows the measured river discharge for this the event.

1



2

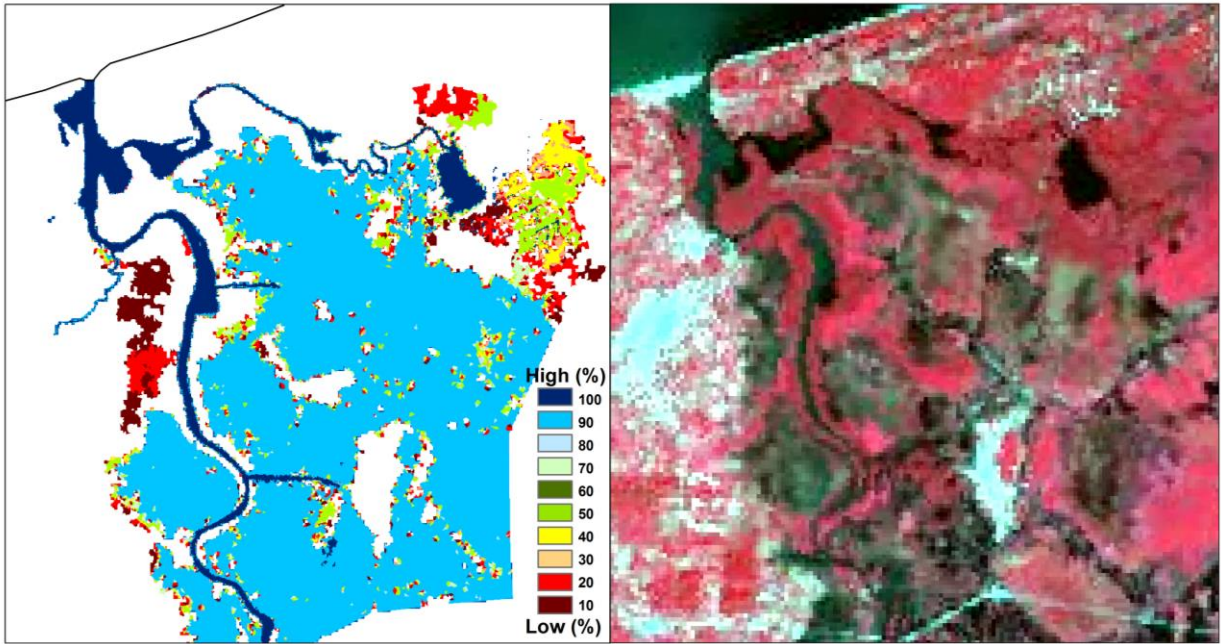
3

**Figure 7.** Model domain along with the numerical mesh and elevation data in the study area; Boundary conditions are represented by blue dot: Agua Dulcita river; red dot: input hydrograph; yellow dot: river-mouth.

5

6

1  
2  
3  
4  
5

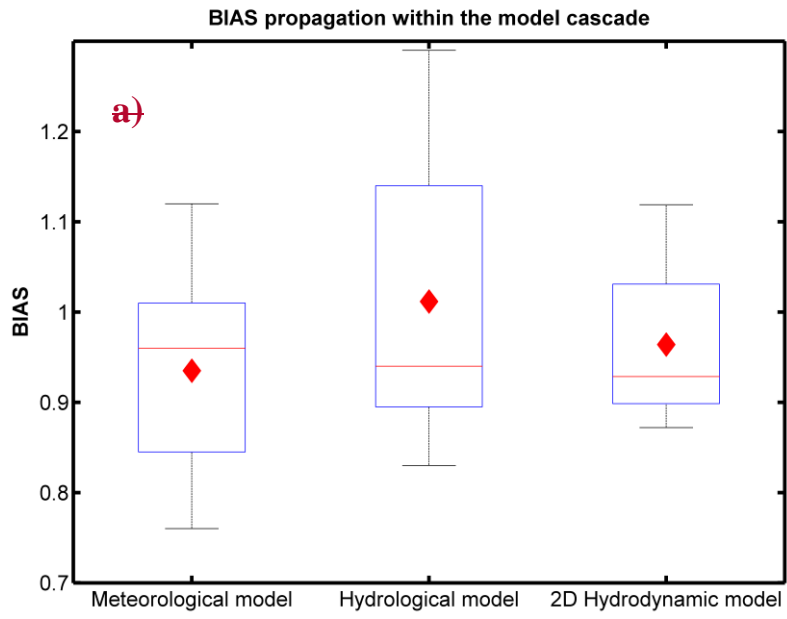


6  
7  
8  
9  
10

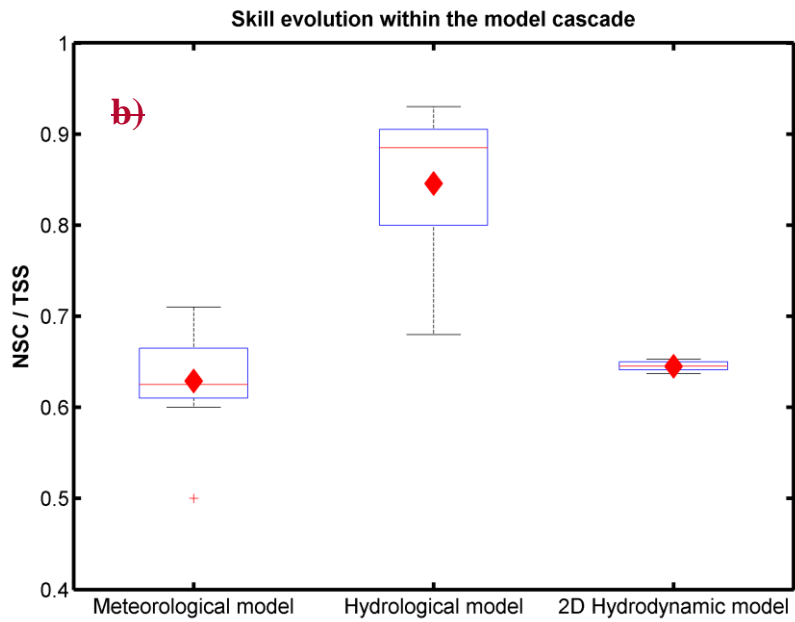
**Figure 8.** Data vs. model comparison of flood extent; a) Probabilistic flood map derived from the ensemble runs with the hydrodynamic model; b) Infrared SPOT image corresponding to the 15<sup>th</sup> November 2009.



1



2



3

4

5

6

7

8

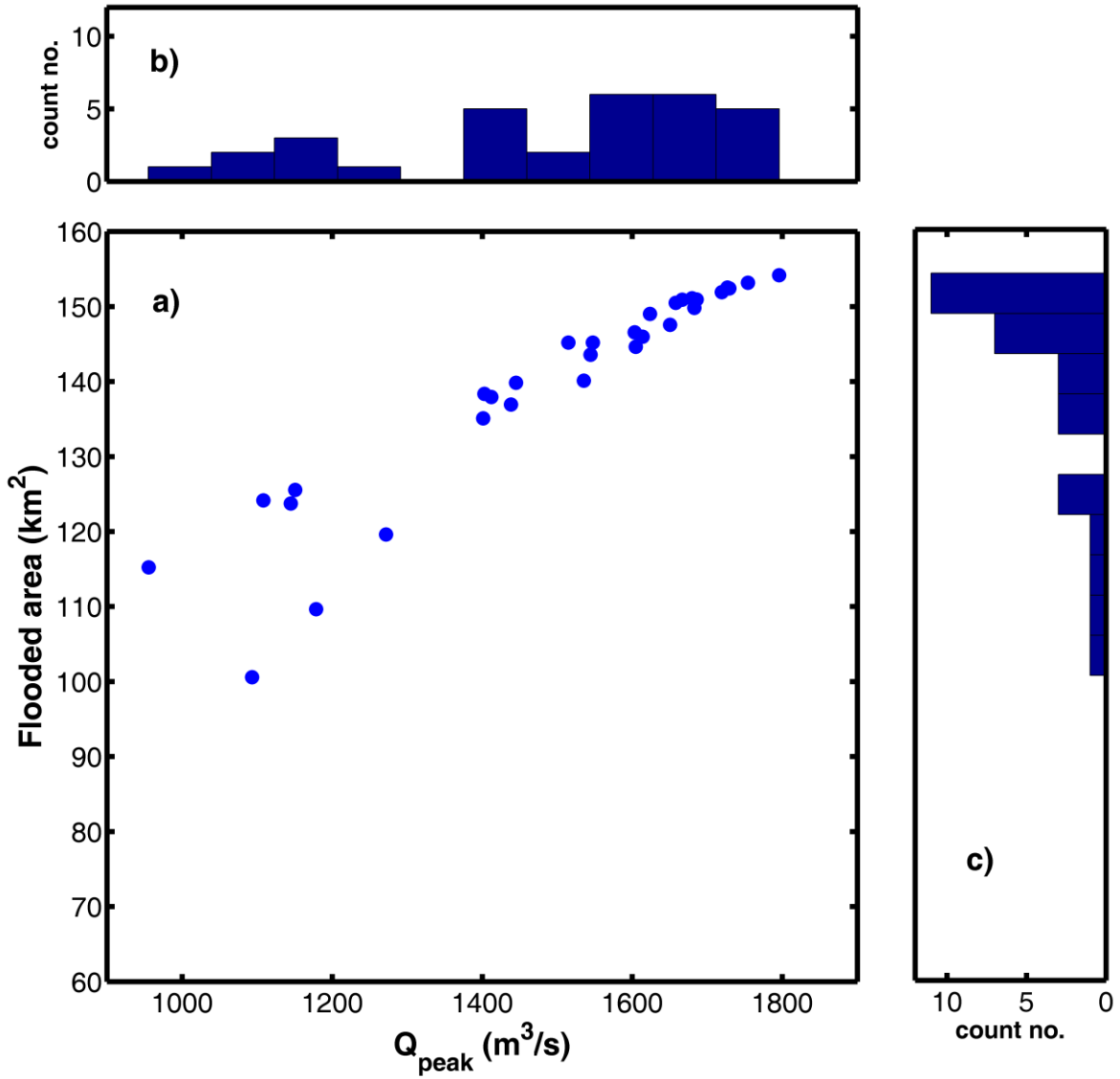
9

10

11

**Figure 9.**

1  
2  
3  
4  
5  
6

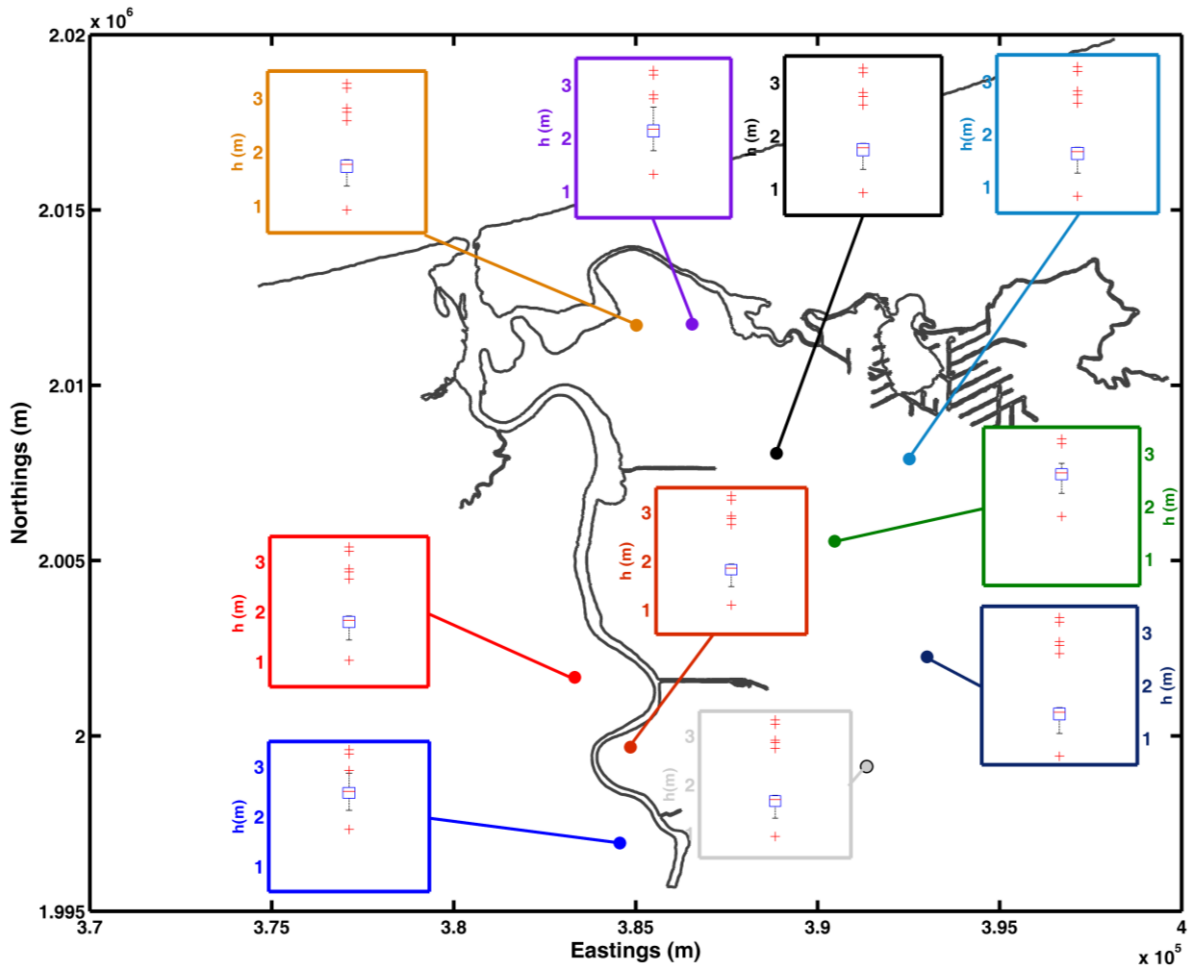


7  
8  
9  
10  
11  
12  
13

**Figure 9.** a) Maximum-flooded area vs. peak discharge estimated for all 31 hydrodynamic simulations of the 2009 flood event; b) Histogram of peak discharges; c) Histogram of estimated size of maximum-flooded area.

| 1  
| 2

1



2

3 **Figure 10.** Estimated maxima inundation depths at different locations within the floodplain.  
4 Red line represents the median. Bars correspond to the standard deviation. Upper and lower  
5 limits of the box are the values of the 25th and 75th , respectively. Crosses depict outliers.

6

7

8

9

10

11

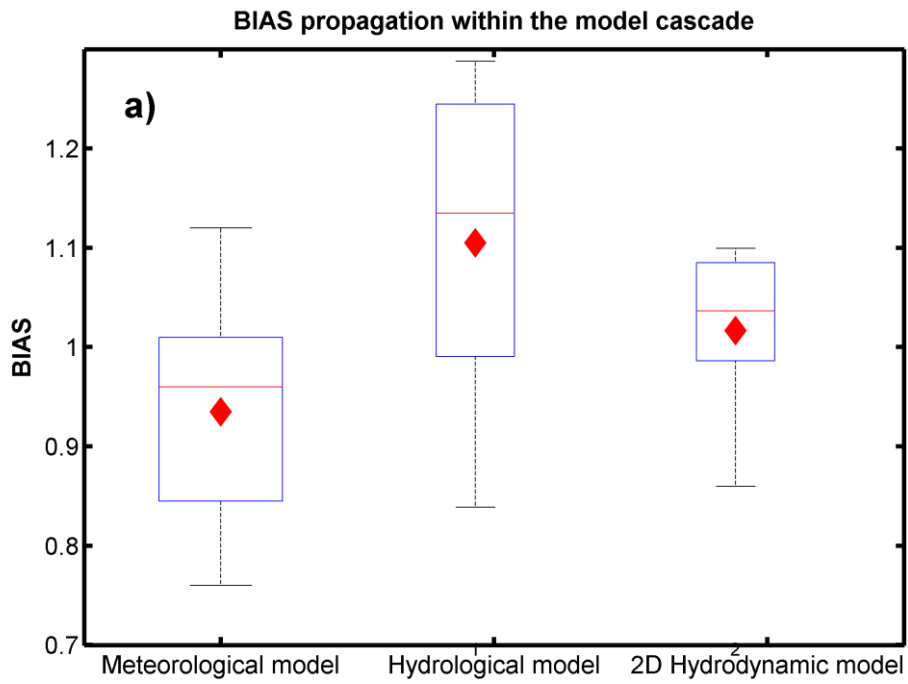
12

13

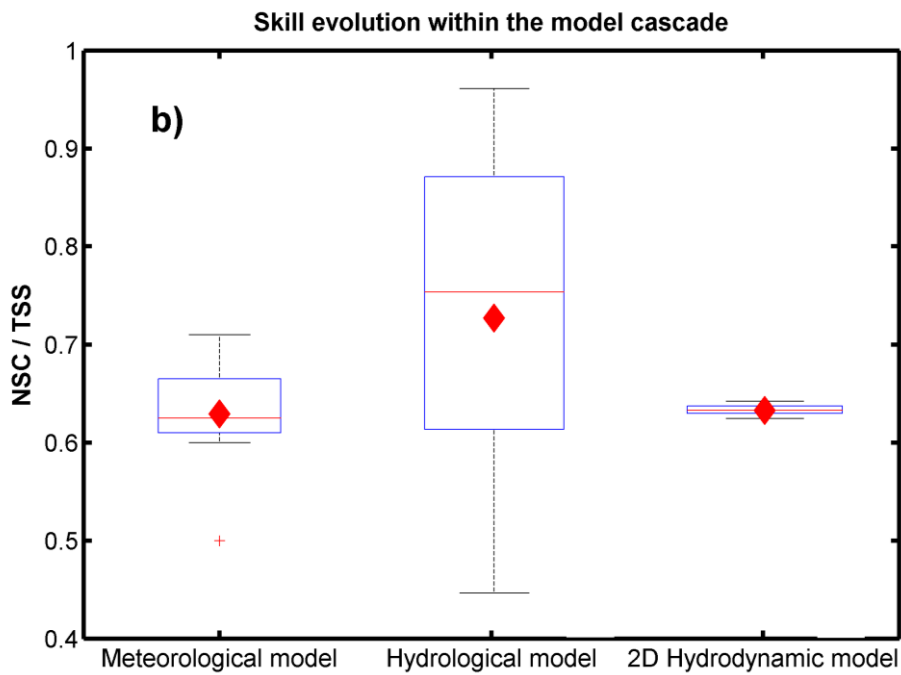
14

15

1



2



3

4

5

**Figure 11.** a) BIAS and b) Skill propagation within the model cascade (meteorological-hydrological-hydrodynamic); diamonds: corresponding ensemble mean value.